Organic LETTERS

Letter

pubs.acs.org/OrgLett

Dragonbloodin A1 and A2: Flavan Trimers and Anti-inflammatory Principles from Sanguis Draconis

Wen-Ke Du,[†] Hsin-Yi Hung,[‡] Ping-Chung Kuo,[‡] Tsong-Long Hwang,[§] Ler-Chun Shiu,[†] Kom-Bei Shiu,[†] E-Jian Lee,[∥] Shih-Huang Tai,[∥] and Tian-Shung Wu*[,‡,⊥]

[†]Department of Chemistry, National Cheng Kung University, 701 Tainan, Taiwan

[‡]School of Pharmacy, National Cheng Kung University Hospital, College of Medicine, National Cheng Kung University, 701 Tainan, Taiwan

[§]Graduate Institute of Natural Products, College of Medicine, Chang Gung University, Research Center for Industry of Human Ecology and Graduate Institute of Health Industry Technology, Chang Gung University of Science and Technology, Department of Anesthesiology, Chang Gung Memorial Hospital, Taoyuan 333, Taiwan

[∥]Departments of Surgery and Anesthesiology and Institute of Biomedical Engineering, National Cheng Kung University, Medical Center and Medical School, Tainan 701, Taiwan

[⊥]Department of Pharmacy, Tajen University, Pintung 907, Taiwan

S *Supporting Information*

ABSTRACT: Two flavan trimers, dragonbloodin A1 (**1**) and A2 (**2**), were isolated as diastereomers from sanguis draconis, a traditional Chinese medicine for regulating blood. The structures of **1** and **2** were elucidated by spectroscopic analysis and X-ray diffraction. Possible interactions between **1** and **2** were discussed, and possible biosynthesis pathways were deduced. Compounds **1**, **2**, and their racemic mixture all exhibited inhibition of human neutrophil elastase in a dose-dependent manner.

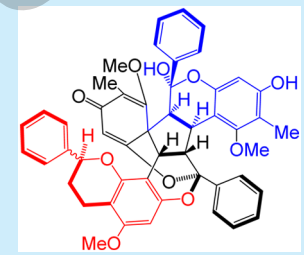

Inflammation plays a key role in many disease conditions, such as Alzheimer's disease, diabetes, infection, psoriasis, wounds, colitis, arthritis, atherosclerosis, immune diseases, and cancer.[1,2] Costs associated with inflammatory diseases have resulted in a billion dollar global drug market. Sanguis draconis, also known as dragon's blood, is a deep red resin, an important traditional Chinese medicine (TCM) for blood regulation.[3] The source of sanguis draconis for TCM use mainly comes from two genuses: *Daemonorops* (Palmae) in Indonesia, India, and Malaysia and *Dracaena* (Liliaceae) in Hainan province of China, Vietnam, and Cambodia.[3] Currently, *Daemonorops draco* (Willd.) Blume from Indonesia is the most common available species for Chinese medicinal formulas.[4] The pharmacological studies on *Daemonorops draco* are in several fields: anticoagulation,[5−8] antiviral activity,[4] antibacteria,[9] anti-inflammatory,[10] anticancer activity,[11−16] and osteogenic activity.[17] So far, the reported chemical constitutions from *Daemonorops draco* are dracorhodin, nordracorubin, nordracorhodin, dammaradienol, (2*S*)-5-methoxy-6-methylflavan-7-ol, (2*S*)-5-methoxyflavan-7-ol, 2,4-dihydroxy-5-methyl-6-methoxychalcone, 2,4-dihydroxy-6-methoxychalcone, dracooxepine, dracoflavans A, B1, B2, C1, C2, D1, and D2, daemonorol series (A−F), abietic acid, and dehydroabietic acid.[10,18−23] However, studies on the relationship of the chemical constituents and their bioactivities are rare, which drew our attention to investigating novel bioactive compounds from this important TCM. In addition, little progress had been made on the purification of the compounds from dragon's blood through these years, indicating the difficulty and limitation of this field. Our preliminary study showed that the stability of the pure compounds was poor, and many polar bioactive compounds were difficult to purify. However, by means of current technology and chiral columns, two novel bioactive structural complex compounds were isolated and their anti-inflammatory activity was evaluated.

Dragonbloodin A (**1** + **2**) was obtained as colorless needles with mp >270 °C. The molecular formula was established as $C_{50}H_{44}O_{10}$ from HR-ESI-MS (*m*/*z* 805.3005 $[M + H]^+$, calcd 805.3007). But ^1H NMR and ^{13}C NMR showed two sets of signals (ratio = 1:1). An unprecedented skeleton was revealed from X-ray analysis, indicating three flavans with spiro structure. A chiral column (ASTEC CELLULOSE DMP) was used to separate two isomers: dragonbloodin A1 (**1**) and dragonbloodin A2 (**2**).[4]

The molecular formula of optically active dragonbloodin A1 (**1**) was established as $C_{50}H_{44}O_{10}$ from HR-ESI-MS (*m*/*z* 805.3003 $[M + H]^+$, calcd 805.3007 for $C_{50}H_{45}O_{10}$), $[\alpha]^{26}_D$ +42.4 (*c* 0.09, $CHCl_3$). The ECD spectrum of **1** showed two positive Cotton effects at 306 and 271 nm as well as a negative Cotton effect at 249 nm). ^1H NMR spectrum of **1** in $CDCl_3$ showed the presence of 15 phenyl group protons [δ_H = 7.87 (2H,

Received: March 6, 2016

DOI: 10.1021/acs.orglett.6b00593
Org. Lett. XXXX, XXX, XXX−XXX

d, J = 8.2 Hz), 7.57 (2H, t, J = 7.6 Hz), 7.48 (1H, t, J = 7.6 Hz), 7.29−7.30 (1H, m), 7.26−7.28 (5H, m), 7.24−7.26 (2H, m), and 7.18 (2H, d, J = 7.6 Hz)], two additional aromatic ring protons [δ_H = 6.35 and 6.06 (each 1H, s)], an α-proton of enone [δ_H = 5.68 (1H, s)], a phenolic OH [δ_H = 4.93 (1H, s, br)], one *O*-linked proton [δ_H = 4.78 (1H, dd, J = 10.4, 2.4 Hz)], four cyclopentane protons [δ_H = 3.96, 3.31 (each 1H, d, J = 4.7 Hz), and 3.85, 3.72 (each 1H, d, J = 9.1 Hz)], three methoxy groups [δ_H = 3.70, 2.94, and 2.65 (each 3H, s)], a hemiacetal OH [δ_H = 2.53 (1H, s, br)], two methylenes [δ_H = 2.61 (1H, ddd, J = 16.8, 5.6, 3.6 Hz), 2.48 (1H, ddd, J = 17.1, 10.9, 5.6 Hz), and 2.03, 1.68 (each 1H, m)], and two methyl groups [δ_H = 2.06 and 1.23 (each 3H, s)]. Moreover, two methoxy groups (δ_H = 2.94 and 2.65) and one methyl group (δ_H = 1.23) are in particular shielded by the spatially close benzene rings. ^{13}C NMR and DEPT135 spectra of **1** in acetone-d_6 revealed the presence of 50 carbon signals, including a carbonyl (δ_C = 187.7), two *O*-linked β-carbon atoms of enone (δ_C = 171.7 and 164.2), 30 aromatic ring carbon atoms (*O*-linked, *C*-linked, unsubstituted, and phenyl groups), two α-carbon atoms of enone [methyl-substituted (δ_C = 112.6) and unsubstituted (δ_C = 106.3)], three *O*-linked carbon atoms [acetal (δ_C = 104.6), hemiacetal (δ_C = 96.9), and one tertiary carbon (δ_C = 96.9)], a spiro carbon atom (δ_C = 54.7), three methoxy groups (δ_C = 59.2, 59.1, and 55.4), four tertiary carbon atoms of the cyclopentane (δ_C = 51.9, 49.2, 38.5, and 35.8), two methylenes (δ_C = 30.0 and 18.9), as well as two methyl groups (δ_C = 9.4 and 8.42). On the basis of the analysis of the ^{1}H−^{1}H COSY, HSQC, and HMBC spectra, all of the ^{1}H and ^{13}C NMR signals of **1** were assigned as shown in Table S1. Dragonbloodin A1 (**1**) includes three parts: hemiacetal flavan moiety (**1a**), spiro flavan moiety (**1b**), and normal flavan moiety (**1c**).

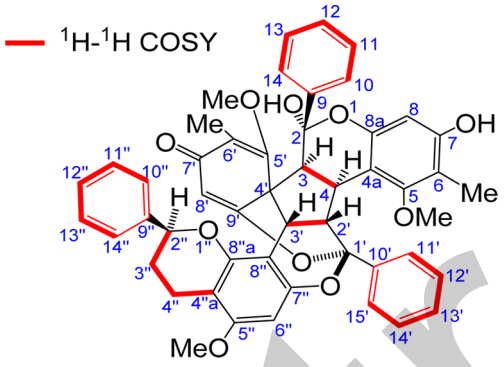

Figure 1. Key ^{1}H−^{1}H COSY correlations of dragonbloodin A1 (**1**).

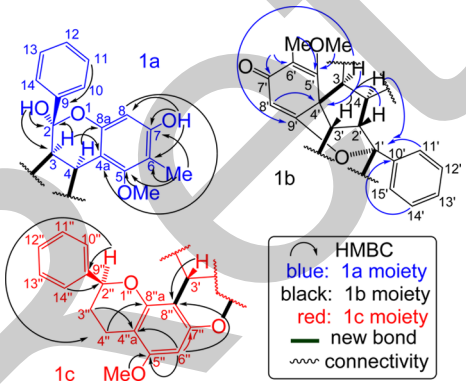

Figure 2. Key HMBC correlations of dragonbloodin A1 (**1**).

The ^{1}H−^{1}H COSY spectrum of **1** showed the presence of six spin systems (C3 to C4, C2′ to C3′, C2″ to C4″, and three phenyl groups; Figure 1). In the HMBC spectrum, the correlations between H3 and C2/C4a, H4 and C8a, H8 and C4a, H11 (H13) and C8a, OH-2 and C2/C3, OMe-5 and C5, Me-6 and C5/C6/C7, as well as between OH-7 and C6/C7/C8 indicated the presence of a hemiacetal flavan moiety (**1a**).The correlations between H2″ and C4″/C9″, H3″ and C4″a, H4″ and C8″a, H6″ and C4″a/C5″/C7″/C8″, H10″/H14″ and C2″ as well as between OMe-5″ and C5″ allowed the establishment of a normal flavan moiety (**1c**). The correlations between H11′/H15′ and C1′, H12′ /H14′ and C10′, OMe-5′ and C5′, Me-6′ and C5′/C6′/C7′ and between H3/H4/H2′/H3′/H8′ and C4′ were indicated for the spiro flavan moiety (**1b**). Moreover, the HMBC correlations also prove that the hemiacetal flavan moiety (**1a**) was connected with the spiro flavan moiety (**1b**) by the correlations between H3 and C9′, and H4 and C1′). The spiro-flavan moiety (**1b**) was linked to a normal-flavan moiety (**1c**) by the correlation between H3′ and C8″ (Figure 2).

Dragonbloodin A2 (**2**) obtained from the cocrystal in chiral system showed the same molecular formula, $C_{50}H_{44}O_{10}$. The ECD spectrum of **2** showed opposite Cotton effects to **1** at 306, 270, and 248 nm. The NMR data of **2** (Table S1) were similar to those of **1** except for protons of OMe-5′, Me-6′, H2″, H3″, H4″,

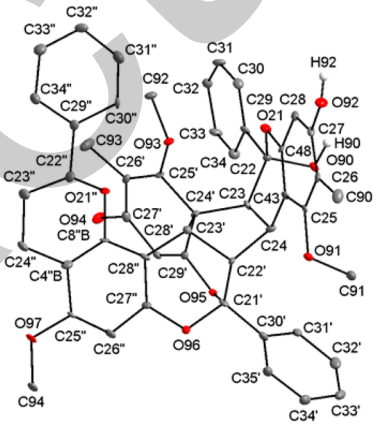

Figure 3. ORTEP diagram of dragonbloodin A1 is presented with thermal ellipsoids for non-hydrogen atoms shown at 15% probability level.

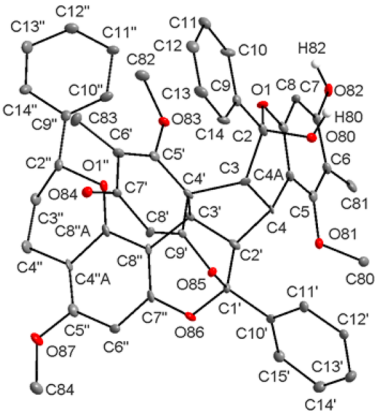

Figure 4. ORTEP diagram of dragonbloodin A1 is presented with thermal ellipsoids for non-hydrogen atoms shown at 15% probability level.

DOI: 10.1021/acs.orglett.6b00593
Org. Lett. XXXX, XXX, XXX−XXX

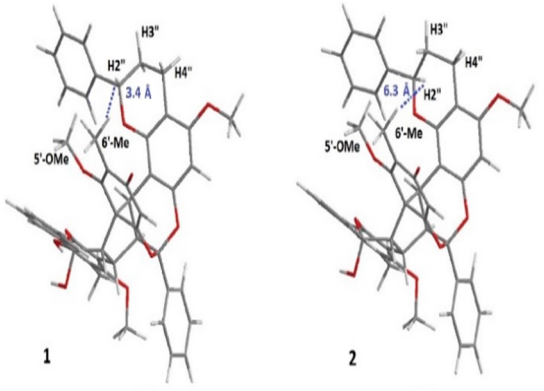

Figure 5. Key differences of the NOESY correlation between **1** and **2**.

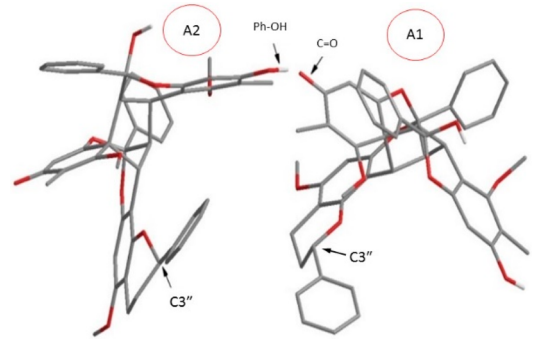

Figure 6. Possible fitting mode between **1** and **2** via hydrogen bonding and the difference of fitting ability from disordered moieties.

and phenyl group of the normal flavan moiety due to intramolecular shielding effects. The carbon signals were also similar to those of **1** except for C2″, C3″, and C4″ on normal flavan moiety due to different conformation.

The stereochemistry of dragonbloodin A1 (**1**) and A2 (**2**) is complicated because there are many permutations and combinations when three flavans integrated. Finally, suitable crystal of dragonbloodin A (**1**+**2**) for single-crystal X-ray diffraction experiment was obtained. The crystal structure can be successfully solved using either $P2_1$ or $P2_1/n$ as the space group. In $P2_1$, a pair of dragonbloodin diastereomers A1 and A2 are found in the asymmetric unit, whereas in $P2_1/n$, the two isomers are merged as one molecule with a carbon atom, which is disordered in two positions at C2″X and C2″Y with occupancies of 0.616 and 0.384, respectively (Figure S1). To emphasize that the single crystals we obtained only contain a pair of isomers, the space group of $P2_1$ was used, producing two ORTEPs for isomers A1 and A2 in Figures 3 and 4, respectively.

Further, the difference between **1** and **2** could be identified via NOESY experiments. The NOE correlation between H2″ and Me-6′ can be observed in **1** not in **2** due to closer spatial distance in **1** (Figure 5). In addition, dracoflavan C_2, a known flavan dimer, was also isolated by us and its ECD spectrum showed negative Cotton effects at 271, 257, and 226 nm.[10] From the combined ECD and NOE data, 2″*S* was assigned to **1**. Thus, the deduced stereocenters of **1** are (2*S*,3*S*,4*S*,1′*R*,2′*S*,3′*R*,2″*S*) and of **2** are (2*S*,3*S*,4*S*,1′*R*,2′*S*,3′*R*,2″*R*). The 2″*S* configuration of **1** can be further verified by upfield shifting of the Me-6′ proton signal (δ_H = 1.17) of **1** due to shilding effects of the phenyl group in normal flavan moiety (Me-6′ δ_H = 0.70 for **2**).

Although pure chiral compounds of **1** and **2** can be obtained, they are very unstable, possibly due to hemiacetal tautomerization in weak acidic or humid conditions (see the Supporting Information). However, the crystal composed of racemic mixture of **1** and **2** is relatively stable. In order to explain this phenomenon, we proposed a pose to address the interaction between two molecules. Hydrogen bonding was proposed between A1 carbonyl group (C7′) and A2 phenolic OH (C7). This pose also imbeds the reactive hemiacetal group, which accounts for its stability (Figure 6).

In this work, compounds **1** and **2** represent the first examples of a new class of flavans with a unique spiro and highly stereospecific backbone. The biosynthesis for **1** and **2** is proposed as shown in Scheme 1.[10,24] Nucleophilic attack of **4** driven by elimination of tertiary alcohol in **5** occurred twice to form flavan

Scheme 1. Proposed Biosynthetic Pathway of 1 and 2

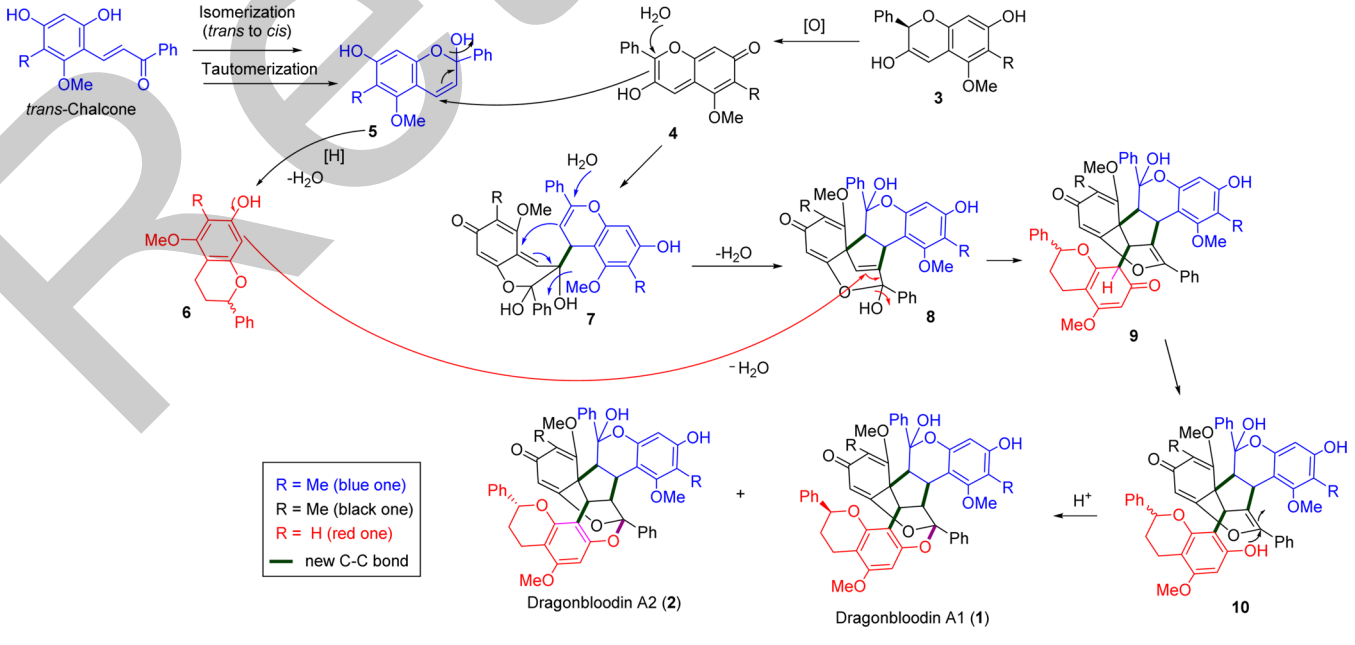

DOI: 10.1021/acs.orglett.6b00593
Org. Lett. XXXX, XXX, XXX−XXX

dimer **8**. Another flavan **6** underwent nucleophilic attack to **8** to form **9**, and a water molecule was eliminated. Aromatization of **9** and final oxygen bridge formation were proposed to give dragonbloodin A1 and A2.

Dragonbloodin A (**1** + **2**), dragonbloodin A1 (**1**), and dragonbloodin A2 (**2**) were evaluated for anti-inflammatory effects on human neutrophil elastase in a cell-free system. IC_{50} of dragonbloodin A for inhibition of human neutrophil superoxide anion generation and elastase release were >10 and 6.53 μM, respectively. In addition, inhibitions of neutrophil elastase release of dragonbloodin A1 and A2 were seen in a dose-dependent manner from 1 to 10 μM (Figures S28 and 29).

■ ASSOCIATED CONTENT

Supporting Information

The Supporting Information is available free of charge on the ACS Publications website at DOI: 10.1021/acs.orglett.6b00593.

Experimental methods, spectroscopic data, X-ray analysis of dragonbloodin A, physiochemical data, and biosynthesis pathways of **1** and **2** (PDF)

X-ray crystallographic data using $P2_1$ as the space group (CIF)

X-ray crystallographic data using $P2_1/n$ as the space group (CIF)

■ AUTHOR INFORMATION

Corresponding Author

*Tel/Fax: +886-6-2747538. E-mail: tswu@mail.ncku.edu.tw.

Notes

The authors declare no competing financial interest.

■ ACKNOWLEDGMENTS

We are thankful to the Ministry of Science and Technology (MOST 103-2113-M006-001), Taiwan, ROC, and Chang Gung Memorial Hospital (CMRPD1B0481-3, CMRPD1D0281-3, and BMRP450 to H.-L.H.) for financial support of the present research

■ REFERENCES

(1) Heneka, M. T.; Carson, M. J.; Khoury, J. E.; Landreth, G. E.; Brosseron, F.; Feinstein, D. L.; Jacobs, A. H.; Wyss-Coray, T.; Vitorica, J.; Ransohoff, R. M.; Herrup, K.; Frautschy, S. A.; Finsen, B.; Brown, G. C.; Verkhratsky, A.; Yamanaka, K.; Koistinaho, J.; Latz, E.; Halle, A.; Petzold, G. C.; Town, T.; Morgan, D.; Shinohara, M. L.; Perry, V. H.; Holmes, C.; Bazan, N. G.; Brooks, D. J.; Hunot, S.; Joseph, B.; Deigendesch, N.; Garaschuk, O.; Boddeke, E.; Dinarello, C. A.; Breitner, J. C.; Cole, G. M.; Golenbock, D. T.; Kummer, M. P. *Lancet Neurol.* **2015**, *14*, 388−405.

(2) Pisoschi, A. M.; Pop, A. *Eur. J. Med. Chem.* **2015**, *97*, 55−74.

(3) *Chinese Herbal Medicine: Materia Medica*, 3rd ed.; Bensky, D., Clavey, S., Stoger, E., Eds.; Eastland Press, 1993.

(4) Gupta, D.; Bleakley, B.; Gupta, R. K. *J. Ethnopharmacol.* **2008**, *115*, 361−80.

(5) Gibbs, A.; Green, C.; Doctor, V. M. *Thromb. Res.* **1983**, *32*, 97−108.

(6) Tsai, W. J.; Hsieh, H. T.; Chen, C. C.; Chen, C. F. *J. Chin. Med.* **1995**, *6*, 59.

(7) Tsai, W.-J.; Hsieh, H.-T.; Chen, C.-C.; Kuo, Y.-C.; Chen, C.-F. *Eur. J. Pharmacol.* **1998**, *346*, 103−110.

(8) Yi, T.; Chen, H.-B.; Zhao, Z.-Z.; Yu, Z.-L.; Jiang, Z.-H. *J. Ethnopharmacol.* **2011**, *133*, 796−802.

(9) Rao, G. S. R.; Gerhart, M. A.; Lee, R. T.; Mitscher, L. A.; Drake, S. *J. Nat. Prod.* **1982**, *45*, 646−648.

(10) Arnone, A.; Nasini, G.; Vajna de Pava, O.; Merlini, L. *J. Nat. Prod.* **1997**, *60*, 971−975.

(11) Xia, M.; Wang, D.; Wang, M.; Tashiro, S.-i.; Onodera, S.; Minami, M.; Ikejima, T. *J. Pharmacol. Sci.* **2004**, *95*, 273−283.

(12) Xia, M.; Wang, M.; Tashiro, S.-i.; Onodera, S.; Minami, M.; Ikejima, T. *Biol. Pharm. Bull.* **2005**, *28*, 226−232.

(13) Xia, M. Y.; Wang, M. W.; Cui, Z.; Tashiro, S. I.; Onodera, S.; Minami, M.; Ikejima, T. *J. Asian Nat. Prod. Res.* **2006**, *8*, 335−343.

(14) He, Y.; Ju, W.; Hao, H.; Liu, Q.; Lv, L.; Zeng, F. *J. Huazhong Univ. Sci. Technol., Med. Sci.* **2011**, *31*, 215−219.

(15) Rasul, A.; Ding, C.; Li, X.; Khan, M.; Yi, F.; Ali, M.; Ma, T. *Apoptosis* **2012**, *17*, 1104−1119.

(16) Yu, J.-h.; Zheng, G.-b.; Liu, C.-y.; Zhang, L.-y.; Gao, H.-m.; Zhang, Y.-h.; Dai, C.-y.; Huang, L.; Meng, X.-y.; Zhang, W.-y.; Yu, X.-f. *Int. J. Med. Sci.* **2013**, *10*, 1149−1156.

(17) Wang, W.; Olson, D.; Cheng, B.; Guo, X.; Wang, K. *J. Ethnopharmacol.* **2012**, *142*, 168−174.

(18) Robertson, A.; Whalley, W. B. *J. Chem. Soc.* **1950**, *0*, 1882−1884.

(19) Nasini, G.; Piozzi, F. *Phytochemistry* **1981**, *20*, 514−516.

(20) Nasini, G.; Arnone, A.; Merlini, L. *Heterocycles* **1989**, *29*, 1119−1125.

(21) Arnone, A.; Nasini, G.; Merlini, L. *J. Chem. Soc., Perkin Trans. 1* **1990**, 2637−2640.

(22) Nakashima, K.-i.; Abe, N.; Kamiya, F.; Ito, T.; Oyama, M.; Iinuma, M. *Helv. Chim. Acta* **2009**, *92*, 1999−2008.

(23) Shen, C.-C.; Tsai, S.-Y.; Wei, S.-L.; Wang, S.-T.; Shieh, B.-J.; Chen, C.-C. *Nat. Prod. Res.* **2007**, *21*, 377−380.

(24) Cardillo, G.; Merlini, L.; Nasini, G.; Salvadori, P. *J. Chem. Soc. C* **1971**, 3967−3970.

DOI: 10.1021/acs.orglett.6b00593
Org. Lett. XXXX, XXX, XXX−XXX

Dragonbloodin A1 and A2 - Flavan Trimers and anti-inflammatory principles from Sanguis Draconis

Wen-Ke Du[†], Hsin-Yi Hung[‡], Ping-Chung Kuo[‡], Tsong-Long Hwang[§], Ler-Chun Shiu [†], Kom-Bei Shiu[†], E-Jian Lee[∥], Shih-Huang Tai[∥], Tian-Shung Wu[‡,⊥,*]

Supporting information

Fig. S19-1. ^{1}H NMR spectrum of **2** in d_6-acetone

Fig. S20. ^{13}C & DEPT-135 NMR spectrum of **2** in d_6-acetone (^{1}H: 700 MHz)

Fig. S21. ^{1}H-^{1}H COSY spectrum of **2** in d_6-Acetone (^{1}H: 700 MHz)

Fig. S22. HSQC spectrum of **2** in d_6-Acetone (^{1}H-^{13}C: 700 MHz)

Fig. S23. HMBC spectrum of **2** in d_6-Acetone (^{1}H-^{13}C: 700 MHz)

Fig. S24. Key NOESY spectrum of **2** in $CDCl_3$ (^{1}H-^{1}H: 700 MHz)

Fig. S25. H2″&6′-Me had NOE (A1, green); had no NOE for A2 (red)

9. Fig. S26. A1 and A2 would transform to other compounds (chiral HPLC)
10. Fig. S27. Biosynthetic pathway of **1** and **2**
11. Fig. S28. Effects of dragonbloodin A1 (**1**) on the activities human neutrophil elastase in cell-free system.
12. Fig. S29. Effects of dragonbloodin A2 (**2**) on the activities human neutrophil elastase in cell-free system.

General Experimental Procedure.

Melting point were determined on Yanaco MP-S3 without temperature corrected. HR-ESI-MS spectra were acquired from VARIAN ProStar LC/VARIAN 901 FT-ICR Mass and Bruker APEX II FT-Mass. Polarimeter were determined on a JASCO P-2000 Polarimeter with 589nm filter. UV spectra were determined on a HITACHI U-0080-D Spectrophotometer with a 0.1 dm length cell. IR spectra were recorded on a PerkinElmer FT-IR Spectrum RX I using KBr pellets. CD spectra were determined on JASCO J-720 Spectropolarimeter. Semi-preparative HPLC (normal phase) was carried out on an SHIMADZU LC-20AT instrument equipped with UV-VIS detector (SHIMADZU, SPD-10A) and a ASTEC CELLULOSE DMP OD-H column (5 μm, 10.0 mm I. D. × 25 cm; SUPELCO, Sigma-Aldrich). 1D and 2D NMR spectra were recorded on Bruker AVIII 400 and AVIII HD 700 spectrometer (1H: 400 and 700 MHz, 13C: 100 and 175 MHz). X-RAY/SCD were recorded on Bruker SMART APEX II Single-Crystal X-Ray Diffractometer with Mo. TLC analyses were carried out using silica gel 60 F_{254} (Merck KGaA). Column chromatography was performed on Geduran Si 60 (40-63 μm, Merck). All solvents used in column chromatography and HPLC were of pesticide residue analysis grade (Fluka, Sigma-Aldrich), analytical grade (J.T. Baker, AVANTOR) and chromatographic grade (MACRON, AVANTOR and Merck), respectively.

Sanguis Draconis collection and compound isolation process

The resin of *Daemonorops draco* was purchased from Chuang Song Zong Pharmaceutical co. Ltd. Taiwan in 2010, and identified by Prof. Chang-Sheng Kuoh, Institute of Biotechnology, National Cheng Kung University. A voucher specimen (Wu-

2010002) was deposited in Department of Pharmacy, National Cheng Kung University, Taiwan.

The resin of *D. draco* (3.0 kg) was thoroughly dissolved in $CHCl_3$ (12.0 L). The insoluble materials were removed by filtration and the filtrate was partitioned with H_2O (6.0 L) to yield $CHCl_3$-soluble fraction (about 3.0 kg) and water-soluble fraction (70 g). The $CHCl_3$-soluble extract (0.5 kg) was subjected to C.C. (Column Chromatography) on a silica gel column with a step gradient (*n*-hexane—acetone 4:1, 2:1, 1:1 and 0:1) to give ten fractions. Fraction 5 (74.3 g) was separated by C.C. on a silica gel column with a step gradient ($CHCl_3$—acetone 49:1, 40:1, 35:1, 29:1, 24:1, 19:1 and 0:1) to give ten fractions: fr. 5-1 (0.1 g), fr. 5-2 (0.1 g), fr. 5-3 (0.2 g), fr. 5-4 (1.6 g), fr. 5-5 (2.2 g), fr. 5-6 (9.6 g), fr. 5-7 (13.2 g), fr. 5-8 (5.4 g), fr. 5-9 (19.3 g) and fr. 5-10 (2.0 g). Fraction 5-7 was separated on a silica gel column with a step gradient (*n*-hexane—acetone 2:1, 7:4, 3:2, 5:4, 1:1, 1:2 and 0:1) to give nine subfractions. Co-crystal of dracoflavan B (6.1 g) was obtained from subfr. 5-7-3. Dragonbloodin A (303 mg) as a co-crystal was obtained between subfr. 5-7-4 and subfr. 5-7-5. Dragonbloodin A1 and A2 were separated by using a ASTEC Cellulose DMP-OD-H chiral column to yield A1 and A2 with *n*-hexane—*i*-PrOH=70:30 as eluent, flow rate=2.1 cm^3 min^{-1}, retention time=16.7 min for A2 (49.5%) and 22.1 min for A1 (50.5%).

X-Ray Crystallography Analysis. Single crystals were grown from CH_2Cl_2/hexane at ambient temperature. Data were collected using a Bruker SMART-CCD diffractometer at 100(2) K. The instrument was equipped with graphite-monochromated Mo K_α radiation (λ = 0.71073 Å). Empirical absorption corrections were made in light of the results of an azimuthal scan. The crystal structure was determined using the direct method and refined using the full-matrix least-squares method on F^2, with all non-hydrogen atoms of the structure refined anisotropically, in SHELXL-97 software.[1] In the structure refinement, the PLATON-SQUEEZE program was applied for the position-disordered solvent (CH_2Cl_2) molecules.[2] All hydrogen atoms were located geometrically with d(C-H) = 0.930 Å and d(O-H) = 0.820 Å. The crystal structure can be successfully solved using either $P2_1$ or $P2_1/n$ as the space group. In $P2_1$, a pair of dragonbloodin diastereomers A1 and A2 are found in the asymmetric unit, whereas in $P2_1/n$, the two isomers are merged as one molecule with a carbon atom, which is disordered in two positions at C2″X and C2″Y with occupancies of 0.616 and 0.384, respectively (Fig. S1). To emphasize that the single crystals we obtained only contain a pair of isomers, the space group of $P2_1$ was used, producing two ORTEPs for isomers A1 and A2 in Figs. 1 and 2, respectively. For quick atomic comparison between two

isomers, the two figures are drawn in a similar orientation with a non-hydrogen atom-to-atom contrast table (Table S1). Crystal data of Dragonbloodin A (1+2) was deposited with the Cambridge Crystallographic Data Centre (CCDC 1401169).

References

1. Sheldrick, G. M. SHELXTL-97; University of Göttingen: Göttingen, Germany.
2. Spek, A. L. *J. Appl. Crystallogr*. **2003**, *36*, 7.

Table S1. A Non-Hydrgoen Atom-to-Atom Contrast Table between Dragonbloodin A1 and Dragonbloodin A2

A1				A2			
C22	C92	C33'	C34"	C2	C82	C13'	C14"
C23	C93	C34'	C43	C3	C83	C14'	C4A
C24	C94	C35'	C48	C4	C84	C15'	C8A
C25	C21'	C22"	C4"B	C5	C1'	C2"	C4"A
C26	C22'	C23"	C8"B	C6	C2'	C3"	C8"A
C27	C23'	C24"	O21	C7	C3'	C4"	O1
C28	C24'	C25"	O21"	C8	C4'	C5"	O1"
C29	C25'	C26"	O90	C9	C5'	C6"	O80
C30	C26'	C27"	O91	C10	C6'	C7"	O81
C31	C27'	C28"	O92	C11	C7'	C8"	O82
C32	C28'	C29"	O93	C12	C8'	C9"	O83
C33	C29'	C30"	O94	C13	C9'	C10"	O84
C34	C30'	C31"	O95	C14	C10'	C11"	O85
C90	C31'	C32"	O96	C80	C11'	C12"	O86
C91	C32'	C33"	O97	C81	C12'	C13"	O87

Table S2. Crystal data

formula	$C_{50}H_{44}O_{10}$
fw (g mol^{-1})	804.85
cryst size (mm^3)	0.65 × 0.43 × 0.31
cryst syst	monoclinic
space group	$P2_1$
a (Å)	15.708(2)
b (Å)	17.744(3)
c (Å)	16.623(3)
α (deg)	90
β (deg)	99.335(2)

γ (deg)	90
V (Å ^{3})	4572.2(12)
Z	4
D_{calc} (g cm^{-3})	1.168
μ, (mm^{-1})	0.081
F(000)	1692.0
reflns collected, unique	21019/13848
R_1/wR_2 (I > 2σ(I))	0.0696/0.1821
GOF on F^2	1.086
largest diff peak and hole (e Å $^{-3}$)	0.392/-0.289

Table S3. Lists of selected bond lengths and angles for Dragonbloodin **A1** and Dragonbloodin **A2**

(a) Bong Lengths (Å):

C2—O1	1.420(6)	C11"—C12"	1.345(7)
C2—O80	1.431(6)	C12"—C13"	1.379(7)
C2—C9	1.516(7)	C13"—C14"	1.316(8)
C2—C3	1.541(6)	C22"—O21"	1.448(4)
C3—C4	1.520(6)	C22"—C23"	1.478(6)
C3—C4'	1.650(7)	C22"—C29"	1.513(6)
C4—C2'	1.518(6)	C23"—C24"	1.516(7)
C4—C4A	1.551(6)	C24"—C4"B	1.500(7)
C5—O81	1.333(6)	C25"—C26"	1.335(7)
C5—C6	1.368(7)	C25"—O97	1.393(6)
C5—C4A	1.431(7)	C25"—C4"B	1.469(7)
C6—C7	1.407(7)	C26"—C27"	1.378(6)
C6—C81	1.506(7)	C27"—O96	1.409(5)
C7—C8	1.371(7)	C27"—C28"	1.412(6)
C7—O82	1.416(6)	C28"—C8"B	1.354(7)
C8—C8A	1.373(7)	C28"—C23'	1.496(6)
C9—C14	1.350(7)	C29"—C34"	1.387(7)
C9—C10	1.387(7)	C29"—C30"	1.404(6)
C10—C11	1.406(7)	C30"—C31"	1.344(8)
C11—C12	1.458(7)	C31"—C32"	1.388(7)
C12—C13	1.293(7)	C32"—C33"	1.356(8)
C13—C14	1.398(7)	C33"—C34"	1.443(8)
C22—O21	1.425(6)	C4"A—C8"A	1.446(7)

C22—O90	1.432(4)	C8"A—O1"	1.273(6)
C22—C23	1.508(7)	C4"B—C8"B	1.349(6)
C22—C29	1.537(6)	C8"B—O21"	1.447(5)
C23—C24'	1.557(6)	C1'—O86	1.394(5)
C23—C24	1.572(7)	C1'—O85	1.429(4)
C24—C43	1.472(7)	C1'—C10'	1.515(7)
C24—C22'	1.566(6)	C1'—C2'	1.575(7)
C25—C43	1.390(7)	C2'—C3'	1.476(7)
C25—C26	1.416(7)	C3'—C4'	1.568(7)
C25—O91	1.423(6)	C4'—C5'	1.427(7)
C26—C27	1.366(7)	C4'—C9'	1.493(8)
C26—C90	1.503(7)	C5'—O83	1.357(6)
C27—O92	1.331(6)	C5'—C6'	1.376(7)
C27—C28	1.399(7)	C6'—C7'	1.523(7)
C28—C48	1.395(7)	C7'—O84	1.205(6)
C29—C30	1.364(7)	C7'—C8'	1.444(7)
C29—C34	1.412(7)	C8'—C9'	1.341(7)
C30—C31	1.386(7)	C9'—O85	1.367(6)
C31—C32	1.321(7)	C10'—C15'	1.331(7)
C32—C33	1.452(7)	C10'—C11'	1.407(6)
C33—C34	1.362(7)	C11'—C12'	1.369(7)
C43—C48	1.389(7)	C12'—C13'	1.420(7)
C48—O21	1.387(6)	C13'—C14'	1.332(8)
C80—O81	1.446(6)	C14'—C15'	1.439(8)
C82—O83	1.431(6)	C21'—O96	1.440(5)
C83—C6'	1.522(9)	C21'—O95	1.447(6)
C84—O87	1.413(6)	C21'—C22'	1.485(5)
C91—O91	1.415(6)	C21'—C30'	1.507(7)
C92—O93	1.441(6)	C22'—C23'	1.578(6)
C93—C26'	1.515(8)	C23'—C24'	1.561(6)
C94—O97	1.447(6)	C24'—C29'	1.501(8)
C2"—O1"	1.460(5)	C24'—C25'	1.569(7)
C2"—C9"	1.507(6)	C25'—C26'	1.339(7)
C2"—C3"	1.542(5)	C25'—O93	1.348(5)
C3"—C4"	1.492(7)	C26'—C27'	1.417(7)
C4"—C4"A	1.498(7)	C27'—O94	1.261(7)
C5"—C4"A	1.324(8)	C27'—C28'	1.451(8)

C5"—O87	1.348(6)	C28'—C29'	1.315(7)
C5"—C6"	1.434(7)	C29'—O95	1.386(6)
C6"—C7"	1.376(7)	C30'—C31'	1.387(6)
C7"—C8"	1.342(7)	C30'—C35'	1.415(7)
C7"—O86	1.363(6)	C31'—C32'	1.417(7)
C8"—C8"A	1.472(6)	C32'—C33'	1.331(7)
C8"—C3'	1.515(5)	C33'—C34'	1.431(7)
C9"—C10"	1.296(7)	C34'—C35'	1.362(8)
C9"—C14"	1.397(7)	C4A—C8A	1.375(7)
C10"—C11"	1.438(8)	C8A—O1	1.375(6)

(b) Bond Angles (deg):

O1—C2—O80	108.4 (4)	C29"—C34"—C33"	118.9 (5)
O1—C2—C9	109.1 (4)	C5"—C4"A—C8"A	120.9 (5)
O80—C2—C9	111.3 (4)	C5"—C4"A—C4"	122.0 (5)
O1—C2—C3	112.2 (4)	C8"A—C4"A—C4"	117.1 (4)
O80—C2—C3	100.9 (4)	O1"—C8"A—C4"A	125.0 (5)
C9—C2—C3	114.7 (4)	O1"—C8"A—C8"	118.7 (4)
C4—C3—C2	113.1 (4)	C4"A—C8"A—C8"	116.3 (4)
C4—C3—C4'	105.4 (4)	C8"B—C4"B—C25"	115.3 (4)
C2—C3—C4'	121.6 (4)	C8"B—C4"B—C24"	126.5 (4)
C3—C4—C2'	104.4 (3)	C25"—C4"B—C24"	118.2 (4)
C3—C4—C4A	111.8 (3)	C4"B—C8"B—C28"	126.4 (5)
C2'—C4—C4A	111.5 (3)	C4"B—C8"B—O21"	118.9 (4)
O81—C5—C6	119.4 (5)	C28"—C8"B—O21"	114.7 (4)
O81—C5—C4A	119.4 (4)	O86—C1'—O85	107.4 (3)
C6—C5—C4A	121.1 (5)	O86—C1'—C10'	108.7 (4)
C5—C6—C7	117.2 (5)	O85—C1'—C10'	107.6 (3)
C5—C6—C81	125.1 (5)	O86—C1'—C2'	108.5 (4)
C7—C6—C81	117.7 (4)	O85—C1'—C2'	110.8 (3)
C8—C7—C6	122.5 (5)	C10'—C1'—C2'	113.6 (4)
C8—C7—O82	119.7 (4)	C3'—C2'—C4	104.2 (3)
C6—C7—O82	117.7 (5)	C3'—C2'—C1'	108.2 (4)
C8A—C8—C7	119.3 (5)	C4—C2'—C1'	112.6 (4)
C14—C9—C10	117.9 (5)	C2'—C3'—C8"	109.9 (3)
C14—C9—C2	121.0 (5)	C2'—C3'—C4'	102.1 (4)

C10—C9—C2	121.1 (5)	C8''—C3'—C4'	113.9 (3)
C9—C10—C11	123.9 (5)	C5'—C4'—C9'	115.1 (5)
C10—C11—C12	114.5 (4)	C5'—C4'—C3'	113.1 (4)
C13—C12—C11	120.0 (5)	C9'—C4'—C3'	107.6 (4)
C12—C13—C14	123.9 (5)	C5'—C4'—C3	118.7 (4)
C9—C14—C13	119.8 (5)	C9'—C4'—C3	100.4 (3)
O21—C22—O90	109.5 (3)	C3'—C4'—C3	100.2 (3)
O21—C22—C23	113.2 (4)	O83—C5'—C6'	124.0 (5)
O90—C22—C23	103.2 (3)	O83—C5'—C4'	109.9 (4)
O21—C22—C29	106.2 (3)	C6'—C5'—C4'	126.1 (5)
O90—C22—C29	108.6 (3)	C5'—C6'—C83	131.8 (5)
C23—C22—C29	116.0 (4)	C5'—C6'—C7'	115.9 (5)
C22—C23—C24'	123.1 (3)	C83—C6'—C7'	112.0 (4)
C22—C23—C24	111.3 (4)	O84—C7'—C8'	121.0 (5)
C24'—C23—C24	104.5 (3)	O84—C7'—C6'	119.8 (5)
C43—C24—C22'	111.0 (4)	C8'—C7'—C6'	119.2 (5)
C43—C24—C23	113.0 (4)	C9'—C8'—C7'	120.8 (4)
C22'—C24—C23	102.6 (4)	C8'—C9'—O85	119.5 (4)
C43—C25—C26	124.1 (5)	C8'—C9'—C4'	122.7 (5)
C43—C25—O91	116.4 (4)	O85—C9'—C4'	117.8 (4)
C26—C25—O91	119.4 (5)	C15'—C10'—C11'	119.7 (5)
C27—C26—C25	117.8 (5)	C15'—C10'—C1'	121.0 (4)
C27—C26—C90	123.4 (5)	C11'—C10'—C1'	119.3 (4)
C25—C26—C90	118.8 (4)	C12'—C11'—C10'	118.7 (4)
O92—C27—C26	117.3 (5)	C11'—C12'—C13'	121.5 (5)
O92—C27—C28	122.0 (5)	C14'—C13'—C12'	118.9 (5)
C26—C27—C28	120.7 (5)	C13'—C14'—C15'	119.4 (6)
C27—C28—C48	119.0 (5)	C10'—C15'—C14'	121.4 (5)
C30—C29—C34	118.8 (5)	O96—C21'—O95	105.6 (4)
C30—C29—C22	123.3 (4)	O96—C21'—C22'	112.1 (3)
C34—C29—C22	117.8 (4)	O95—C21'—C22'	112.9 (3)
C29—C30—C31	117.8 (5)	O96—C21'—C30'	104.3 (4)
C32—C31—C30	125.8 (5)	O95—C21'—C30'	105.9 (4)
C31—C32—C33	117.3 (5)	C22'—C21'—C30'	115.2 (3)
C34—C33—C32	117.8 (5)	C21'—C22'—C24	114.6 (3)
C33—C34—C29	122.5 (5)	C21'—C22'—C23'	107.6 (3)
C48—C43—C25	115.1 (5)	C24—C22'—C23'	103.3 (3)

C48—C43—C24	121.8 (5)	C28"—C23'—C24'	119.0 (3)
C25—C43—C24	123.1 (5)	C28"—C23'—C22'	111.4 (3)
O21—C48—C43	123.2 (4)	C24'—C23'—C22'	96.5 (3)
O21—C48—C28	113.7 (4)	C29'—C24'—C23	105.3 (4)
C43—C48—C28	123.1 (4)	C29'—C24'—C23'	105.7 (4)
O1"—C2"—C9"	111.2 (3)	C23—C24'—C23'	108.2 (3)
O1"—C2"—C3"	107.9 (3)	C29'—C24'—C25'	108.9 (4)
C9"—C2"—C3"	112.0 (3)	C23—C24'—C25'	119.5 (4)
C4"—C3"—C2"	110.5 (4)	C23'—C24'—C25'	108.5 (4)
C3"—C4"—C4"A	112.1 (4)	C26'—C25'—O93	131.5 (4)
C4"A—C5"—O87	116.0 (5)	C26'—C25'—C24'	123.7 (4)
C4"A—C5"—C6"	122.8 (5)	O93—C25'—C24'	104.6 (3)
O87—C5"—C6"	121.1 (4)	C25'—C26'—C27'	120.1 (5)
C7"—C6"—C5"	116.2 (4)	C25'—C26'—C93	124.0 (5)
C8"—C7"—O86	121.6 (4)	C27'—C26'—C93	115.9 (5)
C8"—C7"—C6"	125.0 (5)	O94—C27'—C26'	121.1 (5)
O86—C7"—C6"	113.4 (4)	O94—C27'—C28'	119.6 (4)
C7"—C8"—C8"A	118.7 (4)	C26'—C27'—C28'	119.3 (5)
C7"—C8"—C3'	121.0 (4)	C29'—C28'—C27'	120.5 (4)
C8"A—C8"—C3'	120.2 (3)	C28'—C29'—O95	120.0 (4)
C10"—C9"—C14"	115.6 (4)	C28'—C29'—C24'	125.1 (5)
C10"—C9"—C2"	125.7 (5)	O95—C29'—C24'	113.8 (4)
C14"—C9"—C2"	118.2 (4)	C31'—C30'—C35'	118.7 (5)
C9"—C10"—C11"	125.5 (5)	C31'—C30'—C21'	120.7 (4)
C12"—C11"—C10"	113.1 (5)	C35'—C30'—C21'	120.6 (4)
C11"—C12"—C13"	124.3 (5)	C30'—C31'—C32'	120.7 (5)
C14"—C13"—C12"	117.2 (5)	C33'—C32'—C31'	120.5 (5)
C13"—C14"—C9"	124.0 (5)	C32'—C33'—C34'	119.3 (5)
O21"—C22"—C23"	110.6 (0)	C35'—C34'—C33'	121.3 (5)
O21"—C22"—C29"	106.2 (3)	C34'—C35'—C30'	119.4 (5)
C23"—C22"—C29"	115.8 (3)	C8A—C4A—C5	118.7 (5)
C22"—C23"—C24"	110.7 (4)	C8A—C4A—C4	121.6 (5)
C4"B—C24"—C23"	108.4 (4)	C5—C4A—C4	119.7 (4)
C26"—C25"—O97	126.2 (4)	C8—C8A—C4A	121.0 (5)
C26"—C25"—C4"B	121.2 (5)	C8—C8A—O1	116.1 (4)
O97—C25"—C4"B	112.6 (4)	C4A—C8A—O1	122.9 (4)
C25"—C26"—C27"	118.9 (5)	C8A—O1—C2	116.3 (4)

C26"—C27"—O96	112.7 (4)	C48—O21—C22	115.7 (3)
C26"—C27"—C28"	122.9 (4)	C5—O81—C80	116.0 (4)
O96—C27"—C28"	124.3 (4)	C5'—O83—C82	124.2 (4)
C8"B—C28"—C27"	115.2 (4)	C9'—O85—C1'	119.4 (3)
C8"B—C28"—C23'	127.0 (4)	C7"—O86—C1'	120.7 (4)
C27"—C28"—C23'	117.8 (4)	C5"—O87—C84	122.1 (4)
C34"—C29"—C30"	118.7 (4)	C91—O91—C25	113.5 (3)
C34"—C29"—C22"	119.5 (0)	C25'—O93—C92	122.1 (3)
C30"—C29"—C22"	121.5 (4)	C29'—O95—C21'	117.3 (3)
C31"—C30"—C29"	117.9 (5)	C27"—O96—C21'	116.4 (3)
C30"—C31"—C32"	127.6 (5)	C25"—O97—C94	113.8 (4)
C33"—C32"—C31"	113.7 (5)	C8"A—O1"—C2"	119.4 (4)
C32"—C33"—C34"	123.0 (5)	C8"B—O21"—C22"	113.1 (3)

Fig. S1. An ORTEP diagram of a merged dragonbloodin A (**1**+**2**)molecule is presented with thermal ellipsoids for non-hydrogen atoms shown at 15% probability level. Carbon, oxygen, and hydrogen atoms are shown as gray, red, and white spheres, respectively. All hydrogen atoms except those connected to oxygen atoms are omitted for clarity. The carbon label, C8a, for the atom connected to atoms C8, O1, and C4a, is not shown. One carbon atom was found disordered in two positions with C2"X and C2"Y at occupancies of 0.616 and 0.384, respectively.

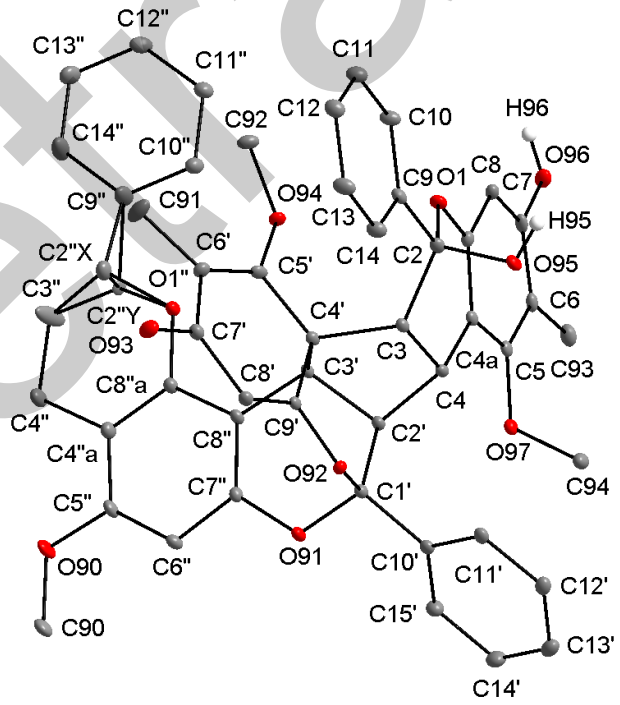

Spectroscopic data of 1 and 2

Table S4 ^{1}H & ^{13}C NMR data of **1** and **2** (*δ* value in ppm, *J* values in Hz). [a]

No.	1		2	
	δ_H	δ_C	δ_H	δ_C
2	-	96.91 (s)	-	96.86 (s)
3	3.90 (d, 9.1)	51.85 (d)	3.86 (d, 9.1)	52.52 (d)
4	3.75 (d, 9.1)	35.81 (d)	3.74 (d, 9.1)	35.49 (d)
4a	-	109.59 (s)	-	109.49 (s)
5	-	157.37 (s)	-	157.51 (s)
6	-	111.36 (s)	-	111.38 (s)
7	-	156.04 (s)	-	156.03 (s)
8	6.40 (s)	100.37 (d)	6.40 (s)	100.57 (d)
8a	-	152.40 (d)	-	152.31 (d)
9	-	143.04 (s)	-	141.45 (s)
10	7.25-7.30 (m)	128.76 (d)	7.14-7.18 (m)	128.80 (d)
11	7.25-7.30 (m)	128.76 (d)	7.14-7.18 (m)	128.80 (d)
12	7.25-7.30 (m)	128.76 (d)	7.14-7.18 (m)	128.80 (d)
13	7.25-7.30 (m)	128.76 (d)	7.14-7.18 (m)	128.80 (d)
14	7.25-7.30 (m)	128.76 (d)	7.14-7.18 (m)	128.80 (d)
2-OH	5.41 (s)	-	5.41 (s)	-
5-OMe	2.93 (s)	59.08 (q)	2.92 (s)	59.08 (q)
6-Me	2.01 (s)	8.42 (q)	1.98 (s)	8.38 (q)
7-OH	8.33 (s)	-	8.28 (s, br)	-
1′	-	104.58 (s)	-	104.52 (s)
2′	3.21 (d, 4.6)	49.20 (d)	3.21 (d, 4.9)	49.56 (d)
3′	4.03 (d, 4.6)	38.49 (d)	3.90 (d, 4.9)	38.40 (d)
4′	-	54.68 (s)	-	54.42 (s)
5′	-	164.17 (s)	-	163.43 (s)
6′	-	112.55 (s)	-	113.02 (s)
7′	-	187.71 (s)	-	187.43 (s)
8′	5.42 (s)	106.30 (d)	5.42 (s)	105.60 (d)
9′	-	171.74 (s)	-	171.89 (s)
10′	-	139.72 (s)	-	139.75 (s)
11′	7.89 (d, 7.4)	127.15 (d)	7.90 (d, 7.4)	127.20 (d)
12′	7.63 (t, 7.7)	128.80 (d)	7.64 (t, 7.7)	128.80 (d)
13′	7.55 (t, 7.7)	129.49 (d)	7.55 (t, 7.7)	129.52 (d)
14′	7.63 (t, 7.7)	128.80 (d)	7.64 (t, 7.7)	128.80 (d)
15′	7.89 (d, 7.4)	127.15 (d)	7.90 (d, 7.6)	127.20 (d)
5′-OMe	2.89 (s)	59.16 (q)	3.20 (s)	58.50 (q)
6′-Me	1.17 (s)	9.24 (q)	0.70 (s)	9.24 (q)
2″	5.02 (dd,9.2, 2.6)	77.64 (d)	5.31 (dd,5.2, 4.0)	77.02 (d)
3″	2.01-2.05 (m)	29.97 (t)	1.98-2.05 (m)	26.56 (t)
	1.71 (m)		1.98-2.05 (m)	
4″	2.53(ddd,16.0, 5.7, 4.6)	18.85 (t)	2.50 (ddd,16.8, 6.2, 4.9)	15.92 (t)
	2.45(ddd,17.2,10.5, 5.9)		1.94-1.98 (m)	
4″a	-	104.22 (s)	-	104.64 (s)
5″	-	158.11 (s)	-	158.15 (s)
6″	6.07 (s)	91.56 (d)	6.10 (s)	91.50 (d)
7″	-	152.83 (s)	-	152.97 (s)
8″	-	100.97 (s)	-	100.80 (s)
8″a	-	153.77 (s)	-	154.07 (s)
9″	-	141.84 (s)	-	142.17 (s)
10″	7.20-7.23 (m)	126.03 (d)	7.05 (d, 7.1)	126.29 (d)
11″	7.20-7.23 (m)	127.70 (d)	7.19-7.24 (m)	127.50 (d)
12″	7.24-7.25 (m)	128.36 (d)	7.19-7.24 (m)	128.25 (d)
13″	7.20-7.23 (d,7.6)	127.70 (d)	7.19-7.24 (m)	127.50 (d)

14″	7.20-7.23 (m)	126.03 (d)	7.05 (d, 7.1)	126.29 (d)
5″-OMe	3.71 (s)	55.38 (q)	3.71 (s)	55.36 (q)

[a] ^{1}H NMR and ^{13}C NMR in d_6-Acetone.

Physico-chemical constants of Dragonbloodin A1 (1) and A2 (2)

Dragonbloodin A1 (**1**). Colorless amorphous powder. Optical rotation ($[\alpha]^{26}_{D}$) +42.3619 (*c* 0.09, $CHCl_3$); UV (logε, in $CHCl_3$) λ_{max} 282.0 (3.84), 247.0 (4.20) nm; IR (KBr) ν_{max} 3372, 2925, 2854, 1667, 1615, 1600, 1448, 1367, 1120, 699 cm^{-1}; ECD (Mol. CD, in $CHCl_3$) 306 (+11.1917), 271 (+2.16617), 249 (-6.10281), 221 (-1.84619), 211 (+0.96840) nm; HR-ESI-MS (m/z 805.3003 $[M+H]^+$, calcd for $C_{50}H_{45}O_{10}$: 805.3007).

Dragonbloodin A2 (**2**). Colorless amorphous powder. Optical rotation ($[\alpha]^{26}_{D}$) -58.0865 (*c* 0.06, $CHCl_3$); UV (logε, in $CHCl_3$) λ_{max} 315.0 (3.26), 283.0 (3.76), 247.0 (4.18) nm; IR (KBr) ν_{max} 3374, 2925, 2854, 1667, 1615, 1601, 1448, 1368, 1121 , 700 cm^{-1}; ECD (Mol. CD, in $CHCl_3$) 306 (-7.79742), 270 (-3.08468), 248 (+5.38757), 222 (-1.24149), 211 (+1.25683) nm; HR-ESI-MS (m/z 805.3007 $[M+H]^+$, calcd for $C_{50}H_{45}O_{10}$: 805.3007).

Fig. S2. Key ^{1}H-^{1}H COSY correlations of Dragonbloodin A1 (**1**)

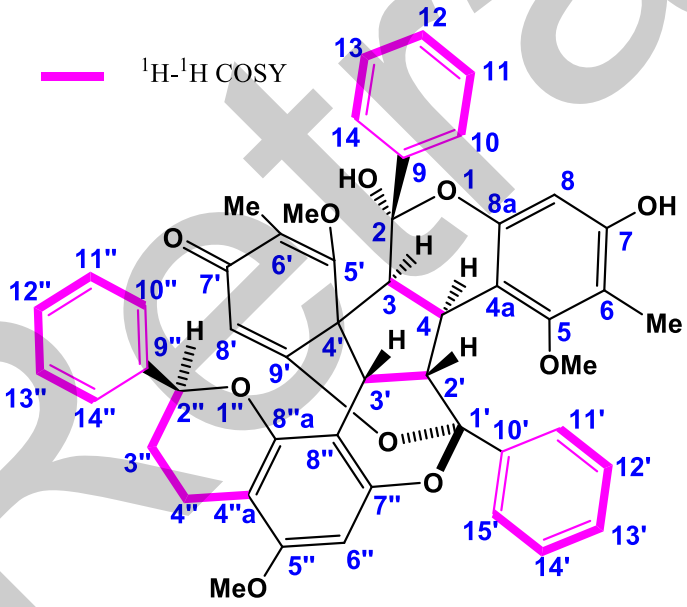

Fig. S3. Key HMBC correlations of Dragonbloodin A1 (1)

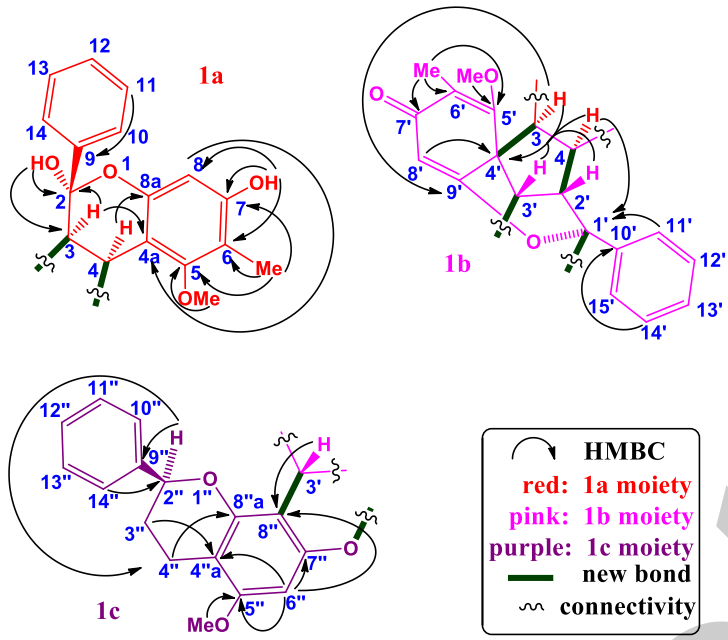

Miscellaneous spectra

Fig. S4. The ECD spectrum of **1** and **2** had opposite peaks to each other.

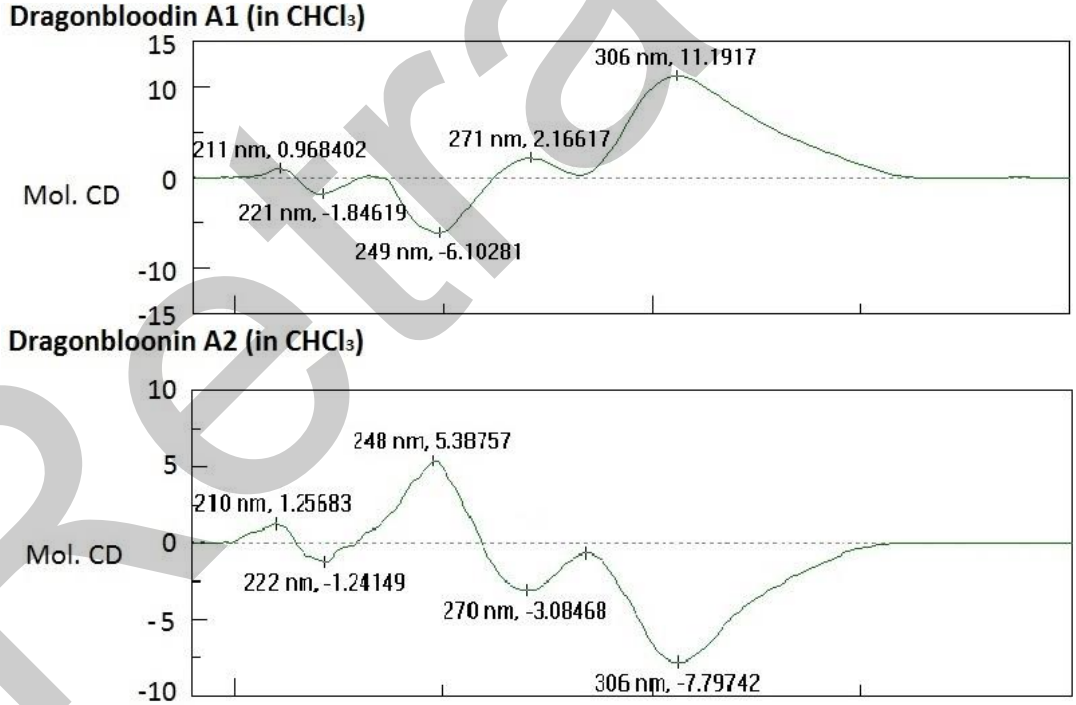

Fig. S5. UV spectrum of 1 in CHCl3

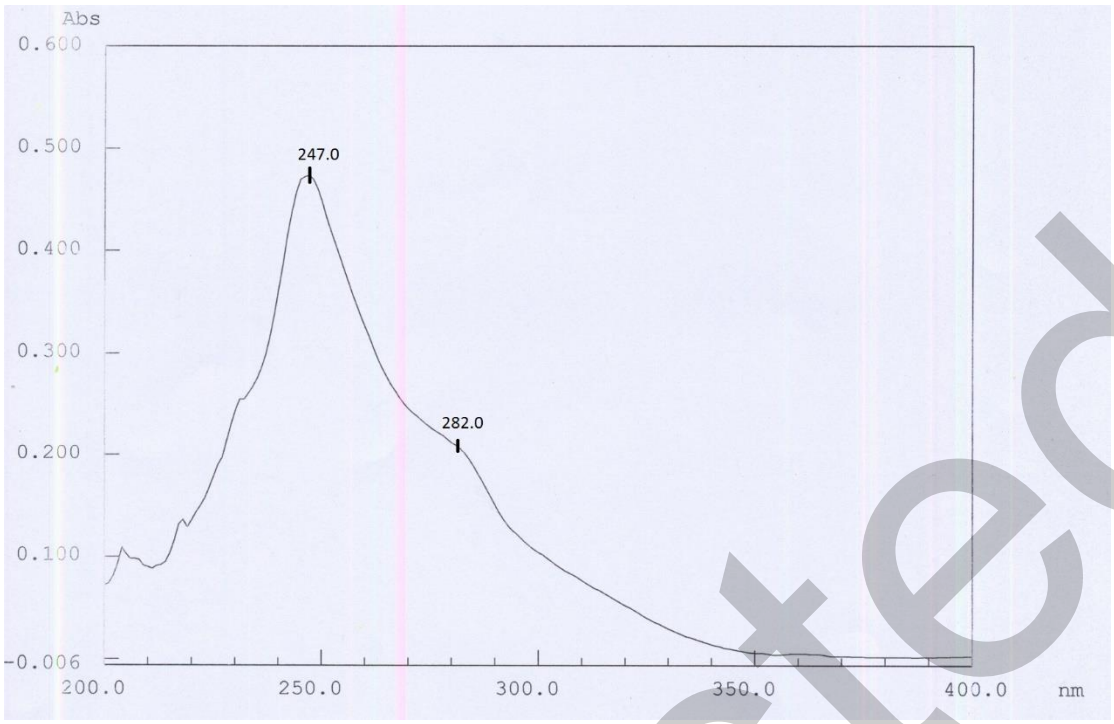

Fig. S6. UV spectrum of **2** in $CHCl_3$

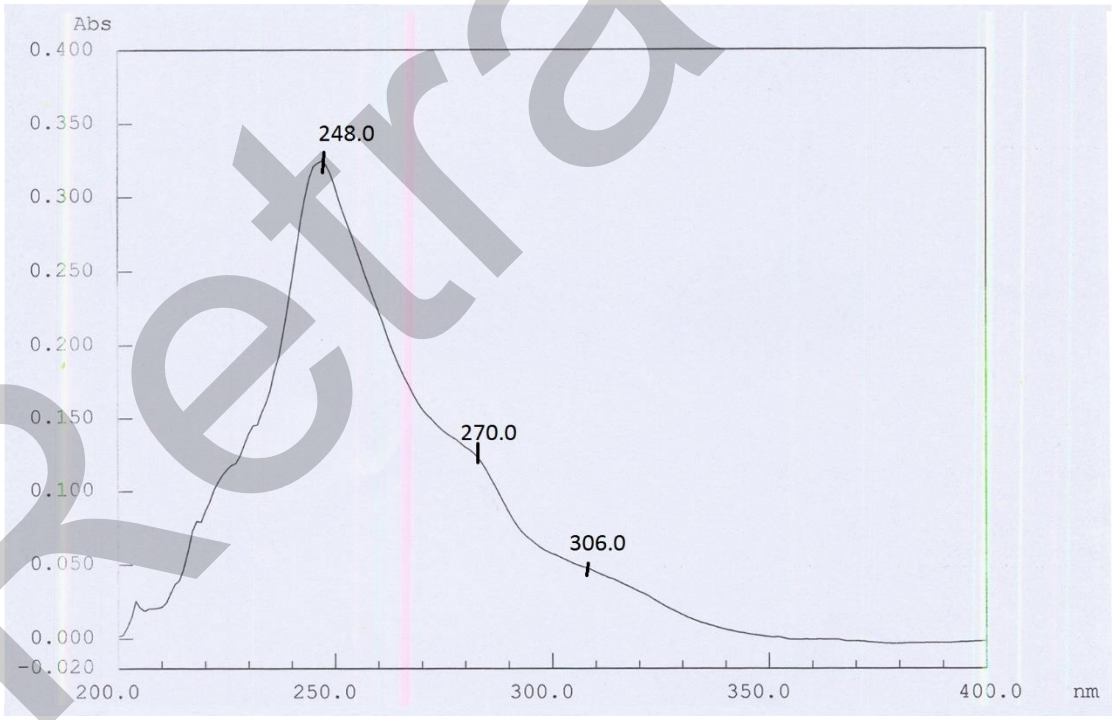

Fig. S7. IR spectrum of 1 (KBr disc)

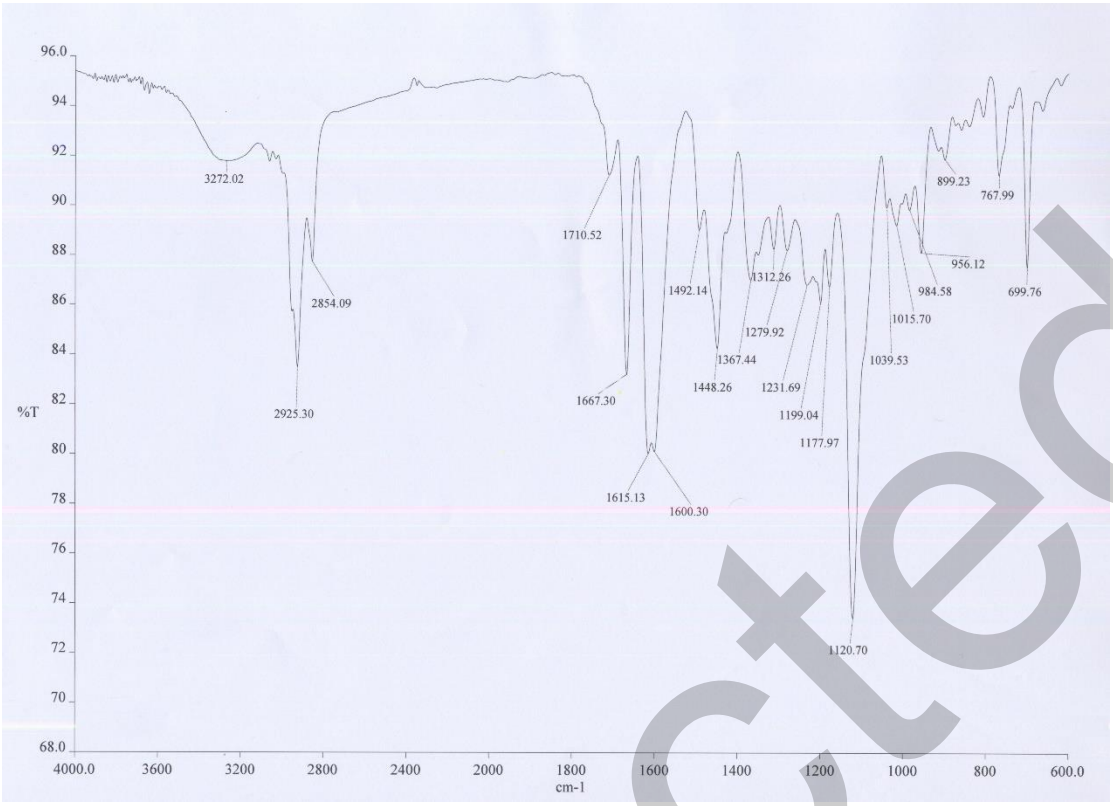

Fig. S8. IR spectrum of **2** (KBr disc)

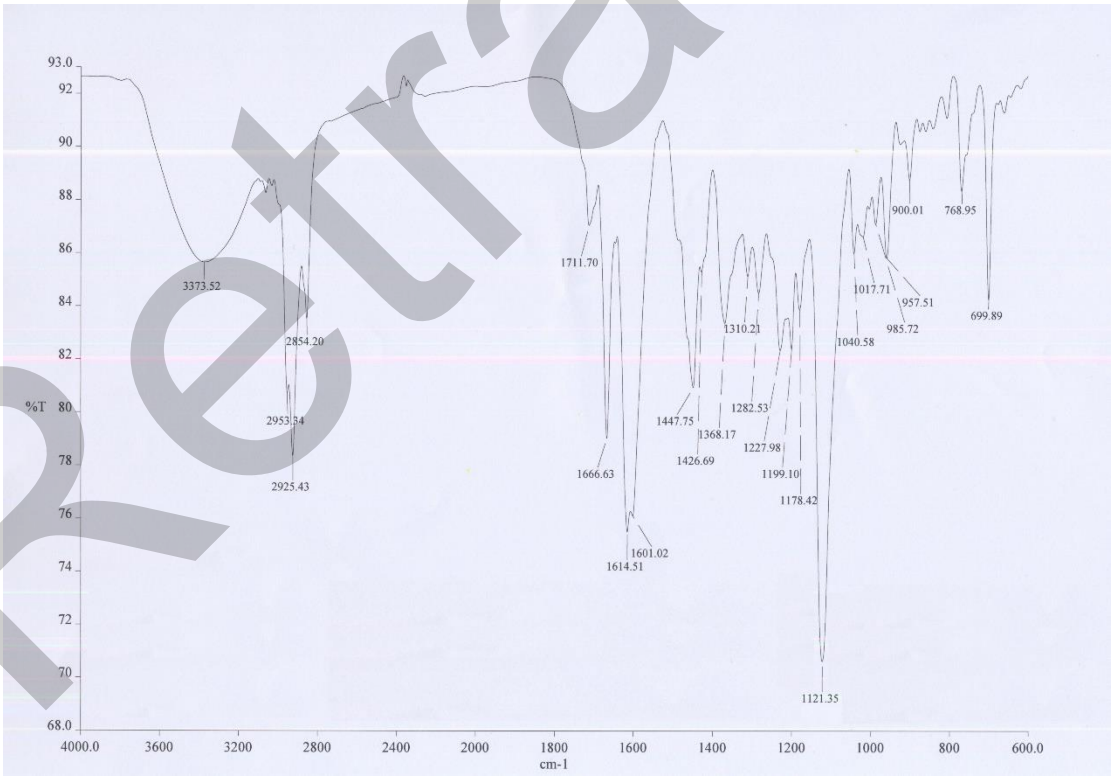

Fig. S9. HR-ESI-Mass of **1**

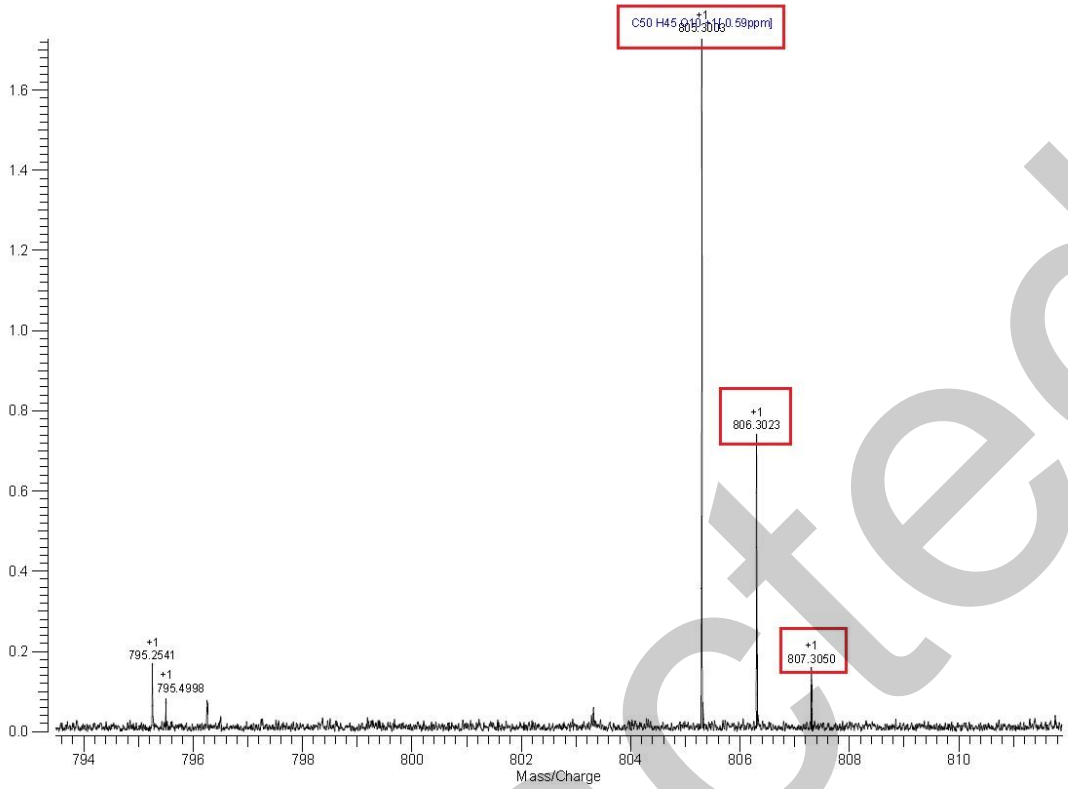

Fig. S10. HR-ESI-Mass of **2**

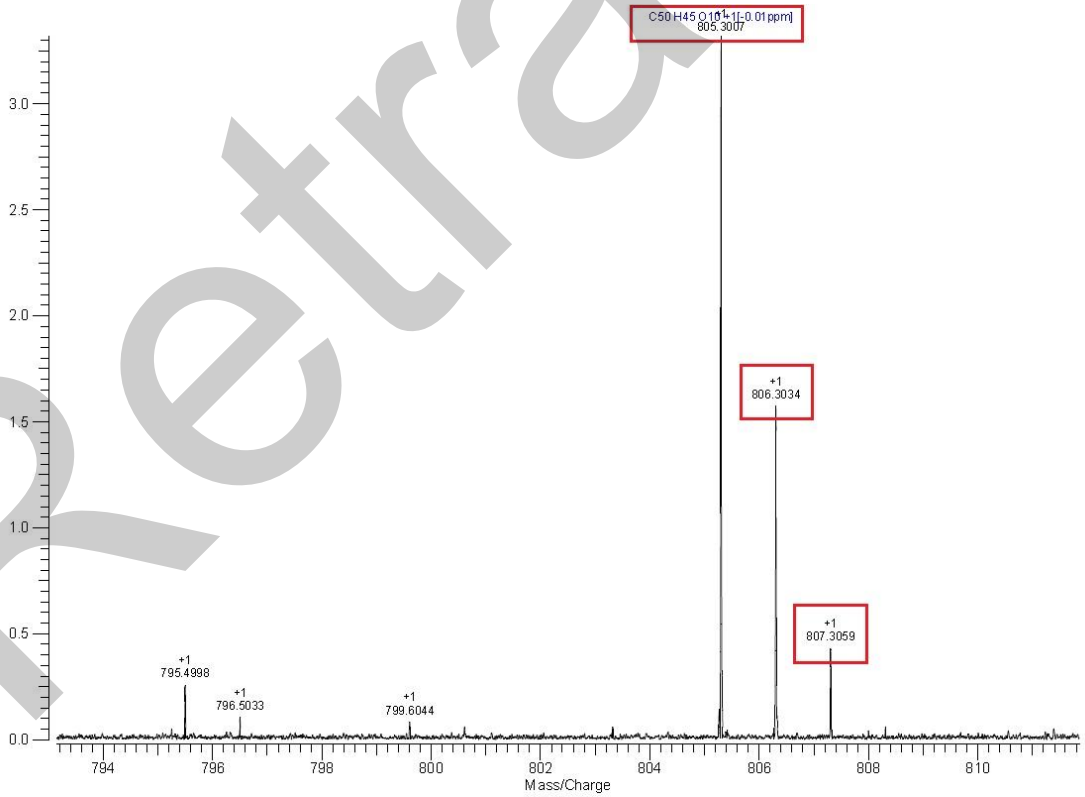

Fig. S11. ^{1}H NMR spectrum of (**1+2**) in $CDCl_3$ (^{1}H: 400 MHz)

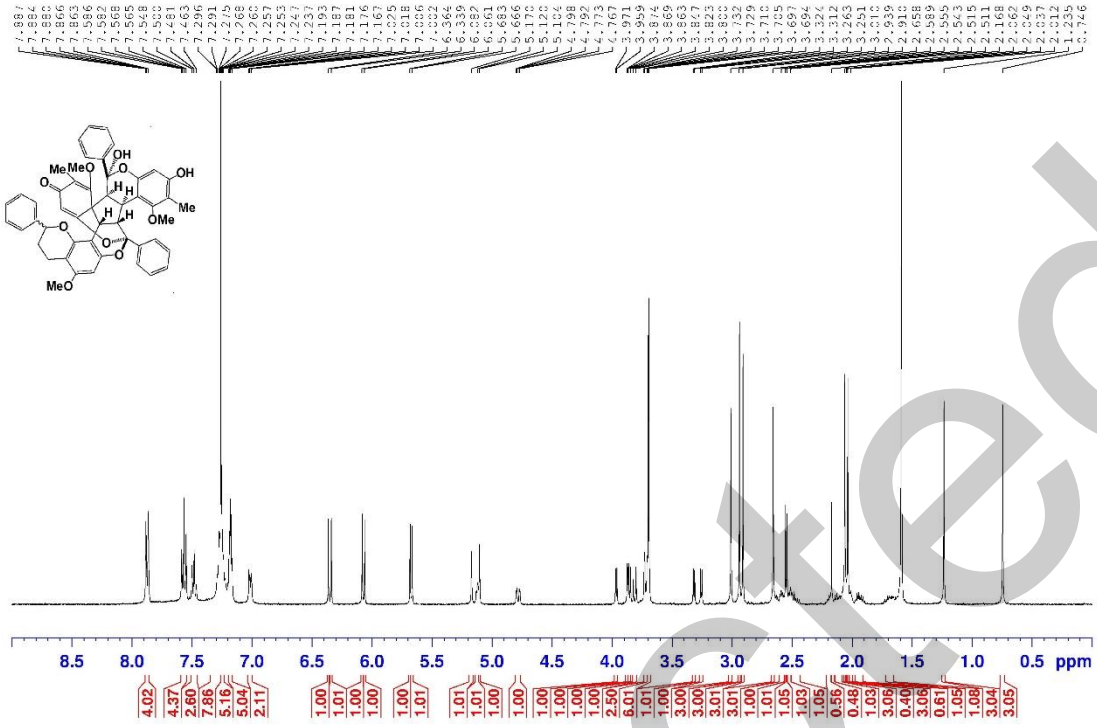

Fig. S12. ^{13}C & DEPT-135 NMR spectrum of (**1+2**) in $CDCl_3$ (^{13}C: 400 MHz)

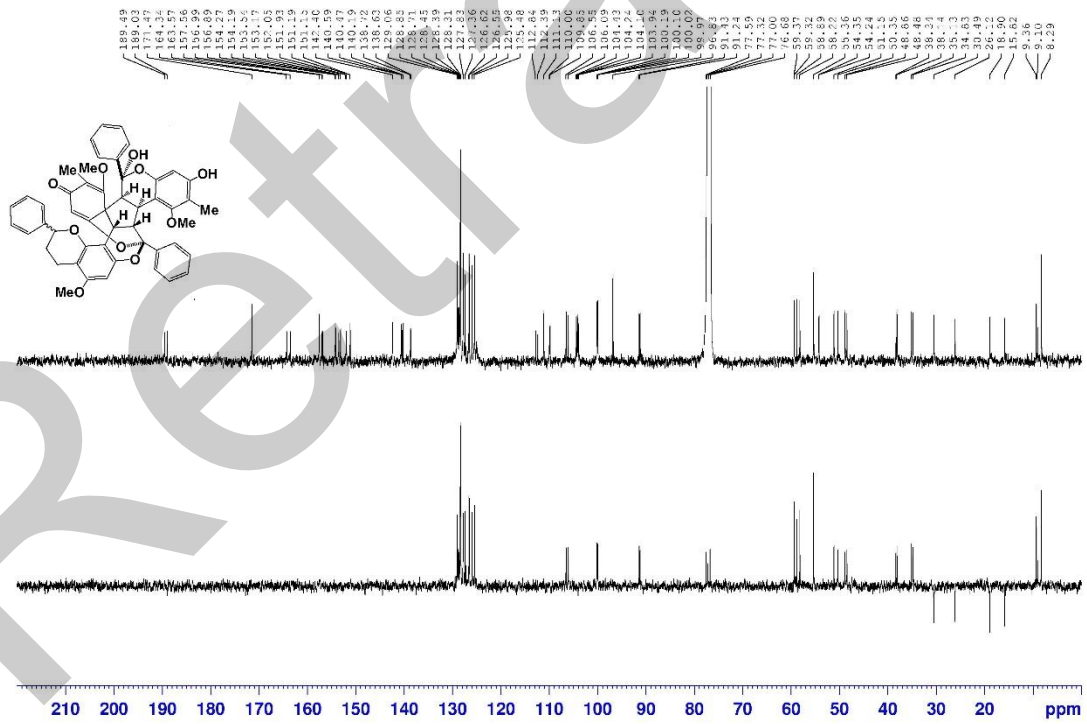

Fig. S13. ^{1}H NMR spectrum of **1** in $CDCl_3$ (^{1}H: 700 MHz)

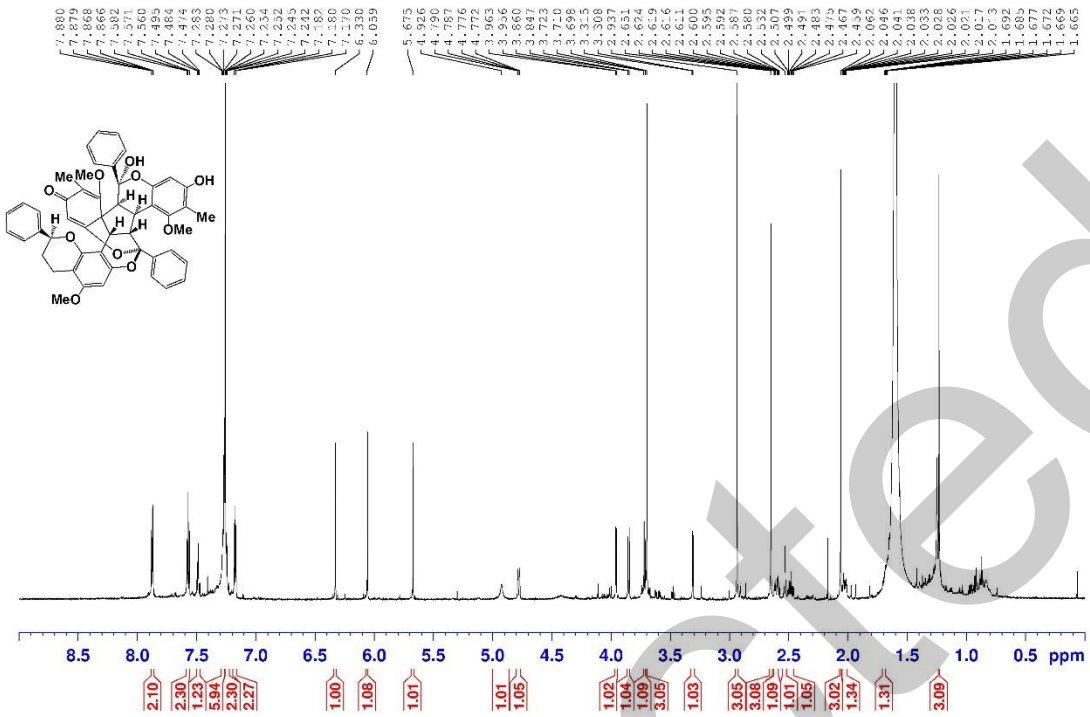

Fig. S13-1.^{1}H NMR spectrum of **1** in d_6-acetone

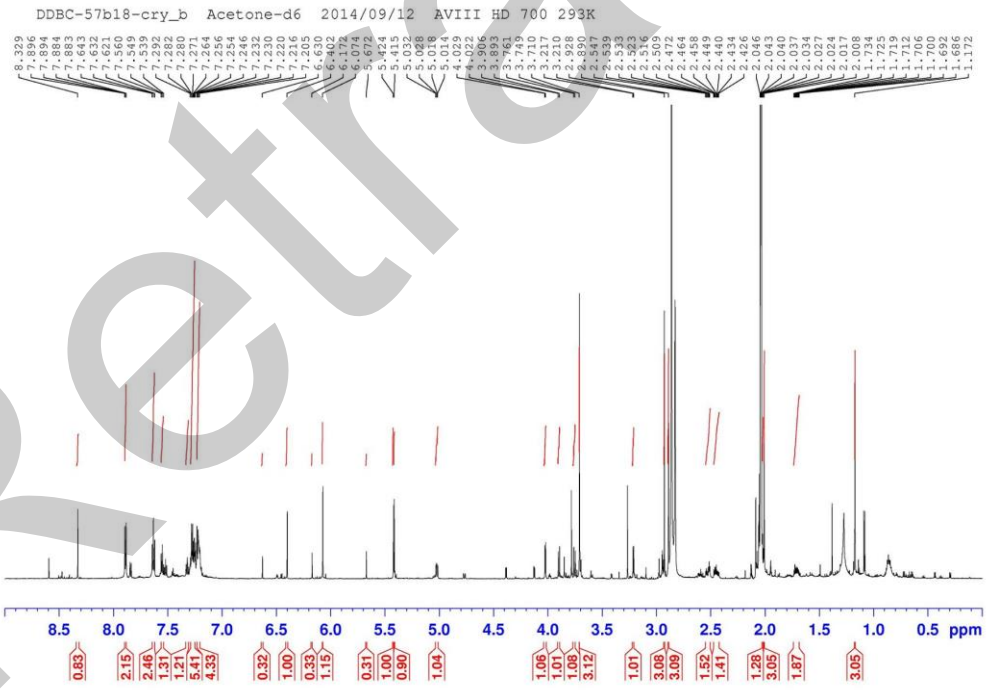

Fig. S14. ^{13}C & DEPT-135 NMR spectrum of **1** in d_6-Acetone (^{13}C: 700 MHz)

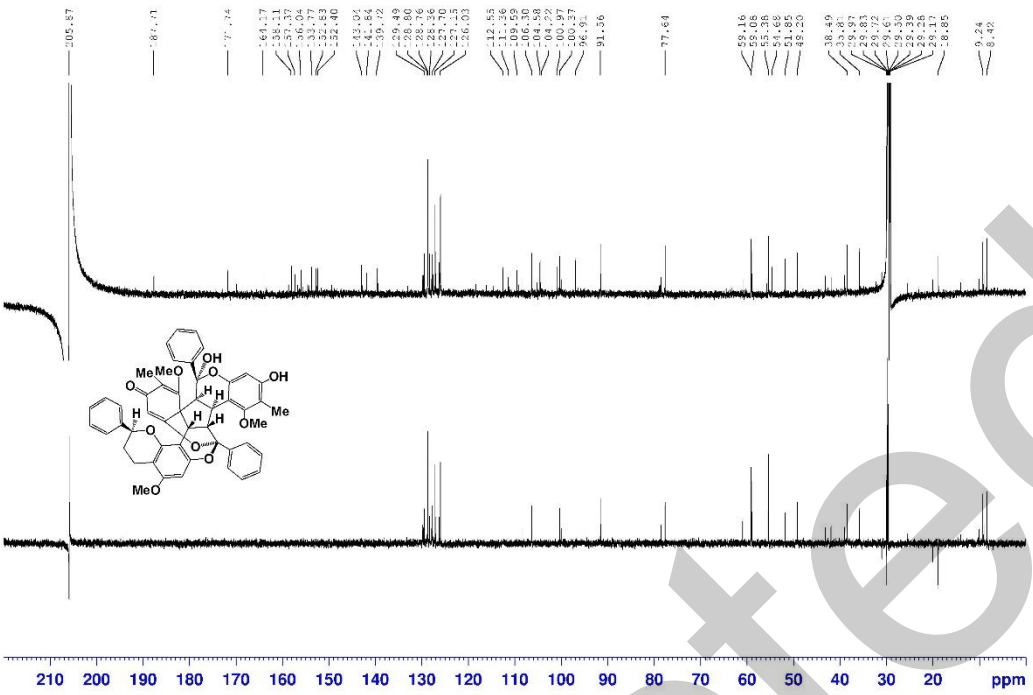

Fig. S15. ^{1}H-^{1}H COSY spectrum of **1** in d_6-Acetone (^{1}H: 700 MHz)

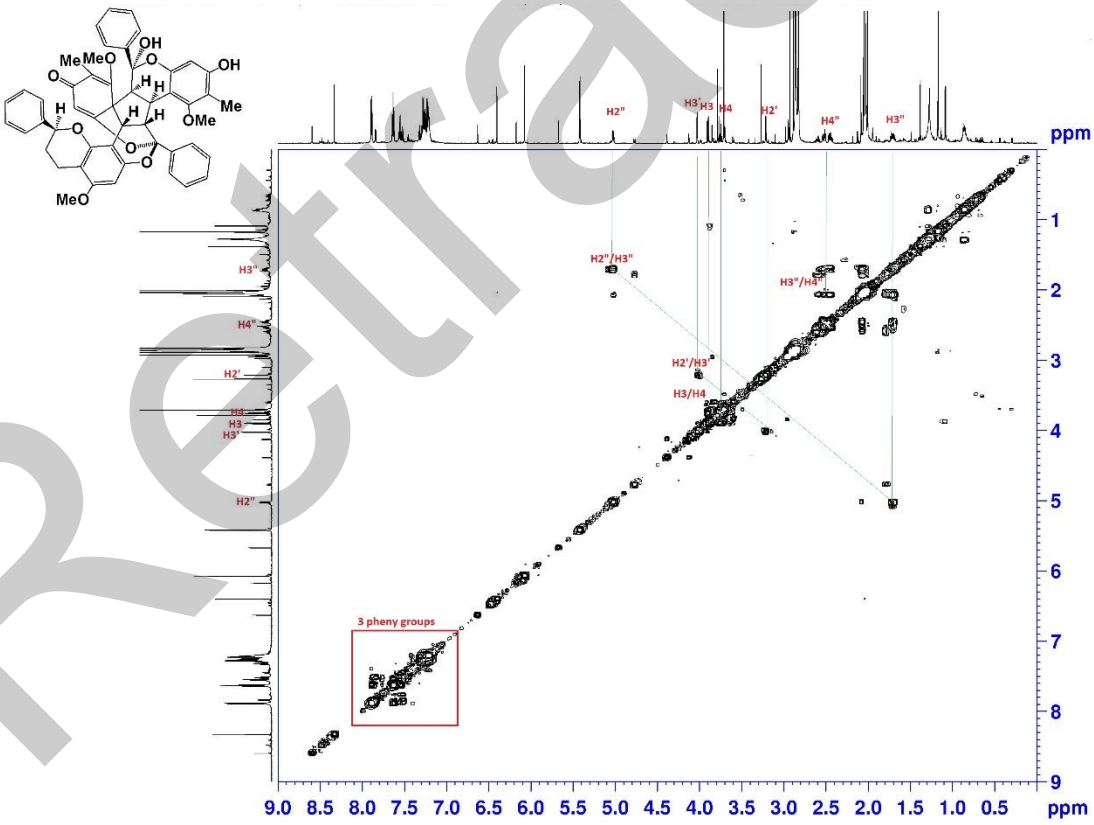

Fig. S16. HSQC spectrum of **1** in d_6-Acetone (^1H-^{13}C: 700 MHz)

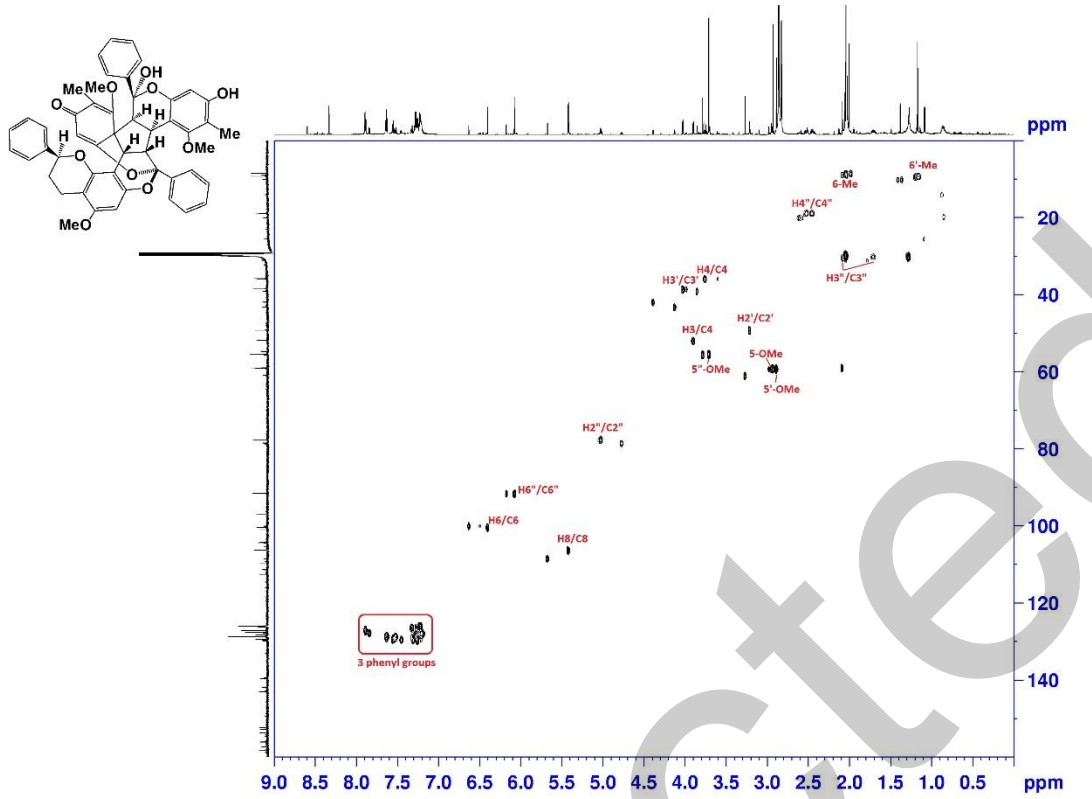

Fig. S17. HMBC spectrum of **1** in d_6-Acetone (^1H-^{13}C: 700 MHz)

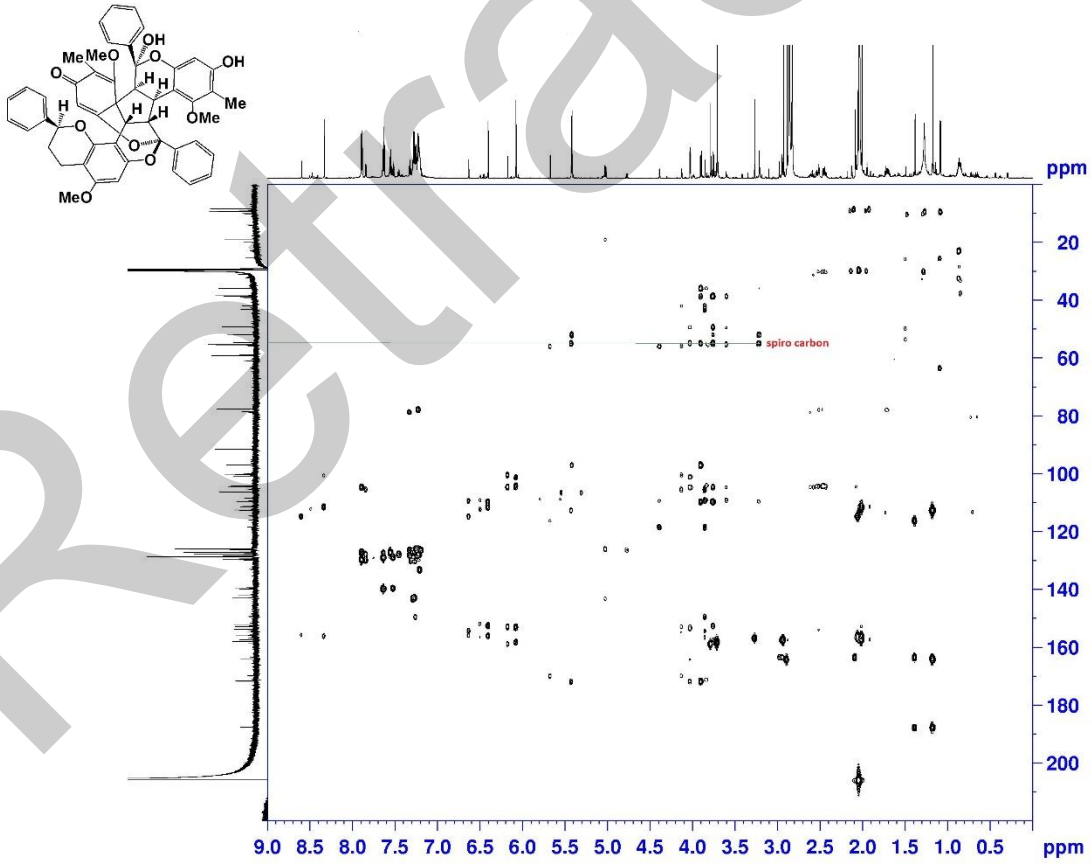

Fig. S18. Key NOESY spectrum of **1** in $CDCl_3$ (^1H-^1H: 700 MHz)

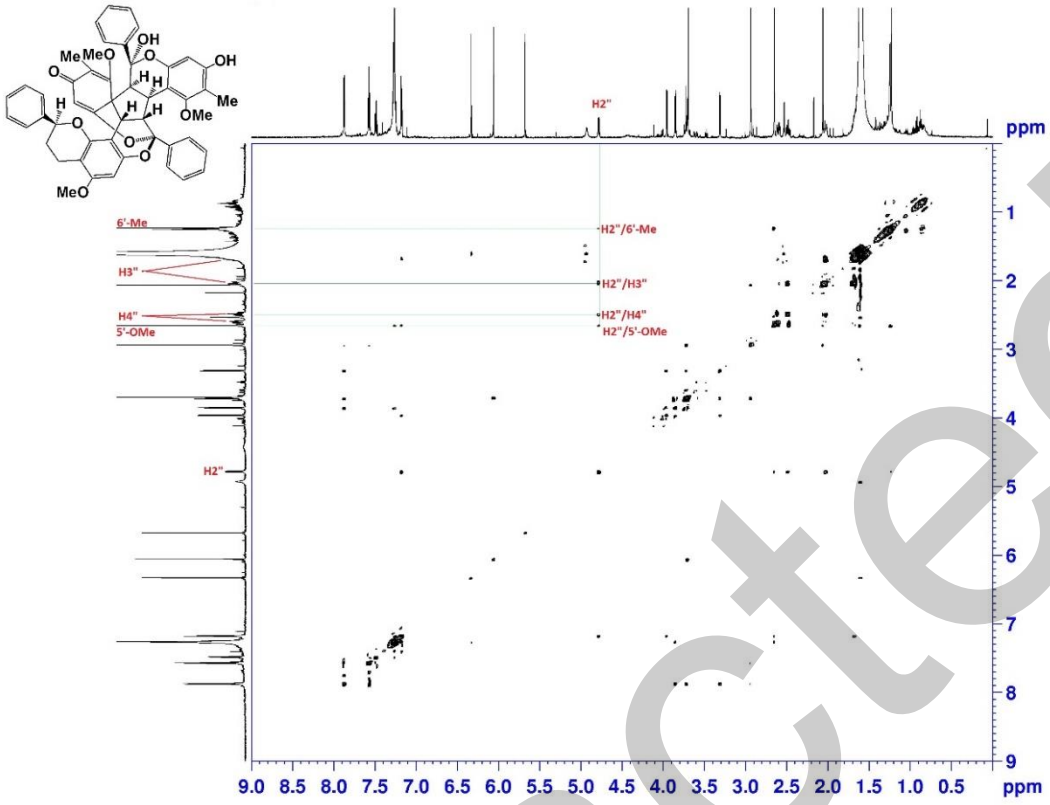

Fig. S19. ^1H NMR spectrum of **2** in $CDCl_3$ (^1H: 700 MHz)

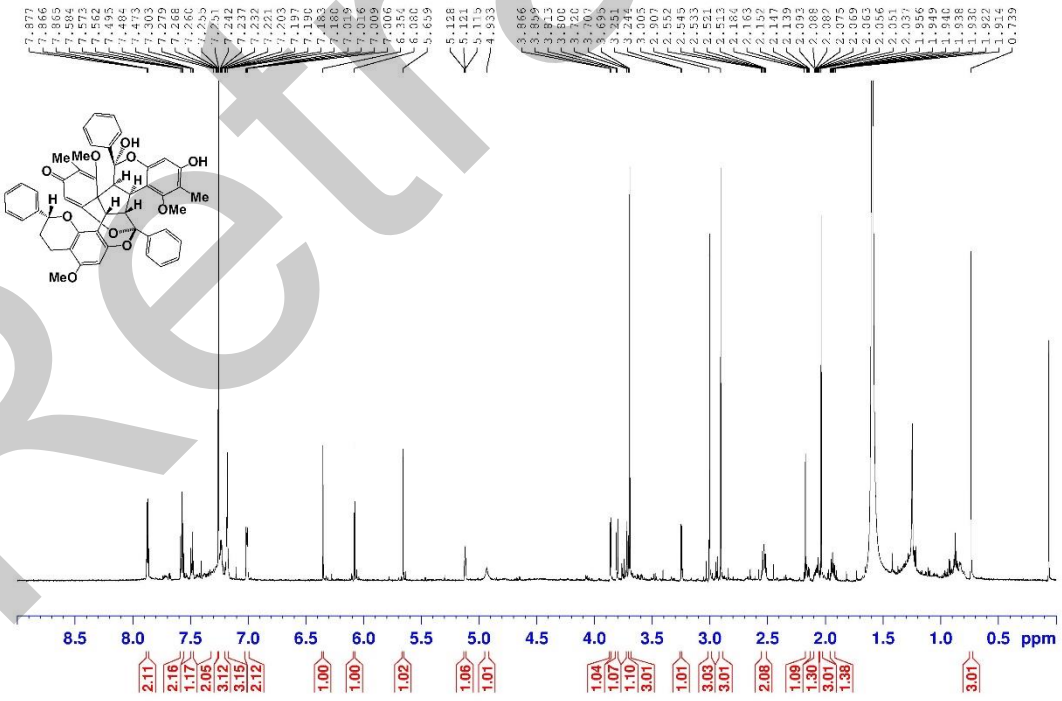

Fig. S19-1. ^{1}H NMR spectrum of **2** in d_6-acetone (^{1}H: 700 MHz).

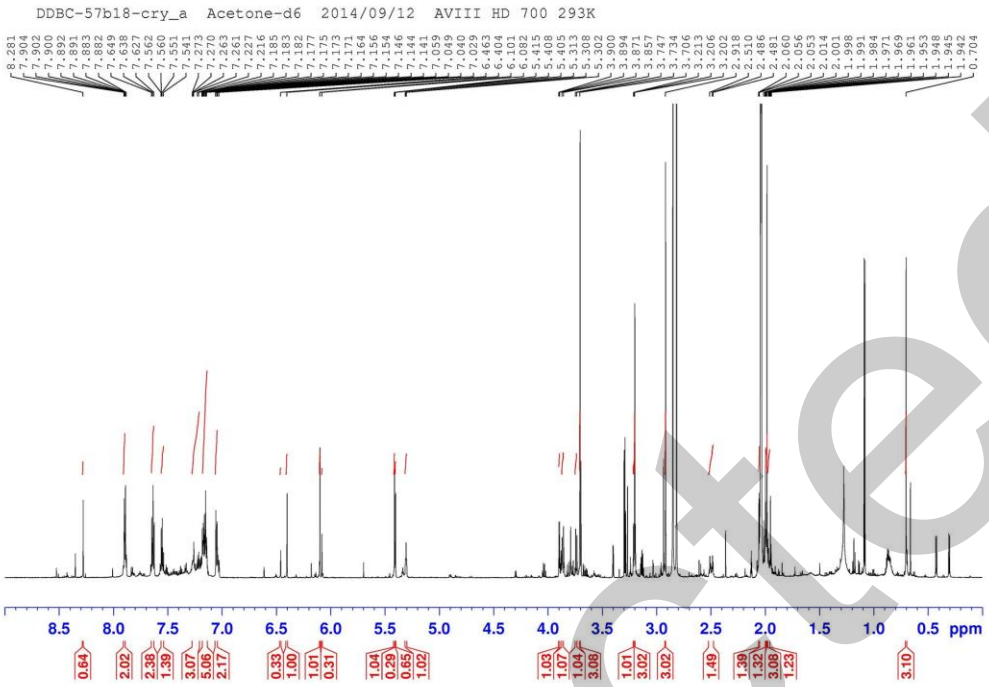

Fig. S20. ^{13}C & DEPT-135 NMR spectrum of **2** in d_6-Acetone (^{13}C: 700 MHz)

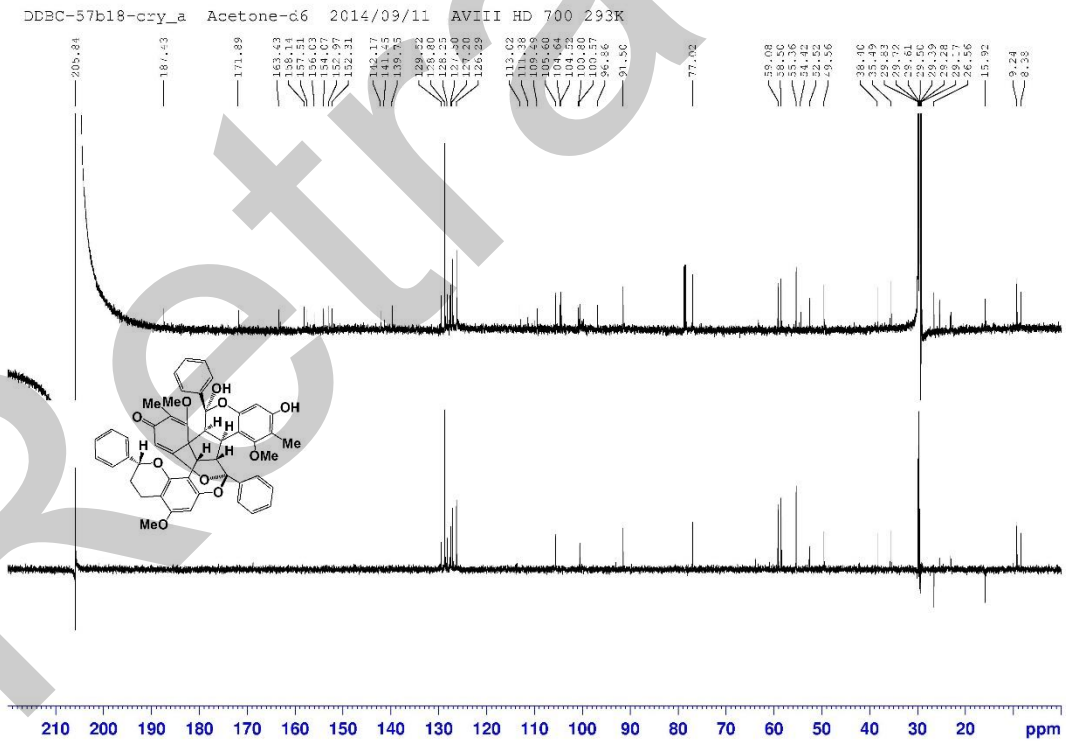

Fig. S21. ^{1}H-^{1}H COSY spectrum of **2** in d_6-Acetone (^{1}H: 700 MHz)

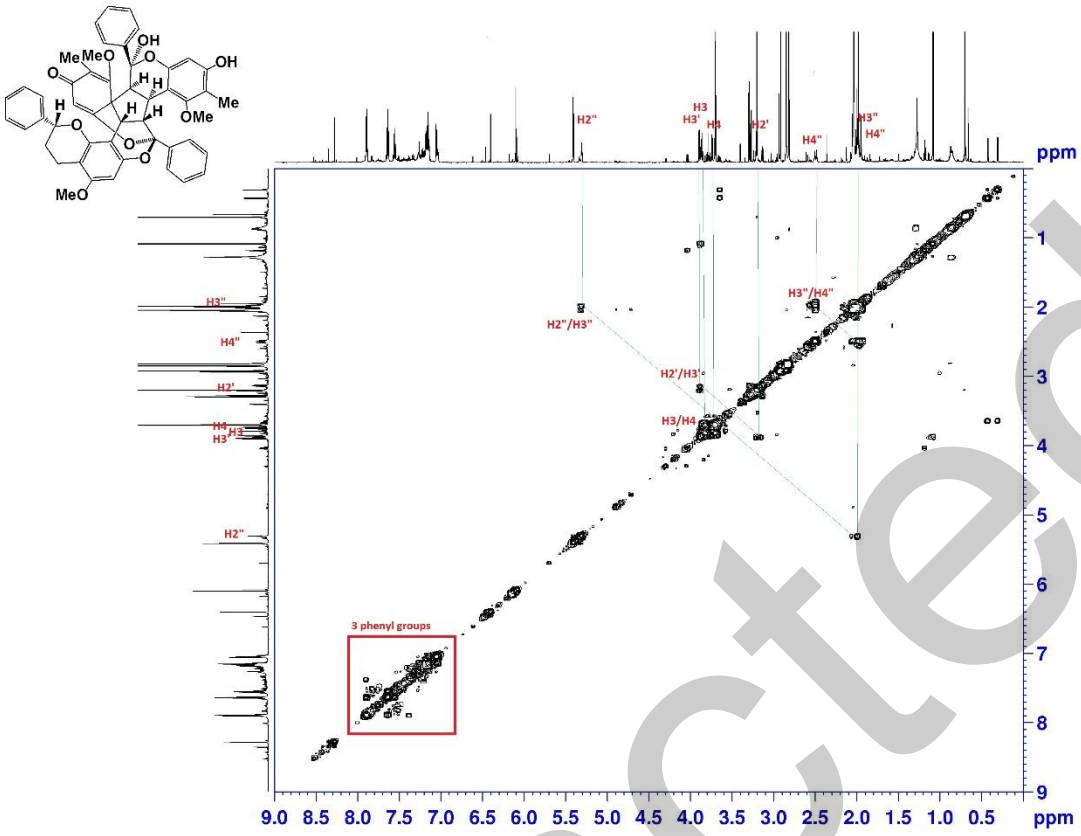

Fig. S22. HSQC spectrum of **2** in d6-Acetone (^{1}H-^{13}C: 700 MHz)

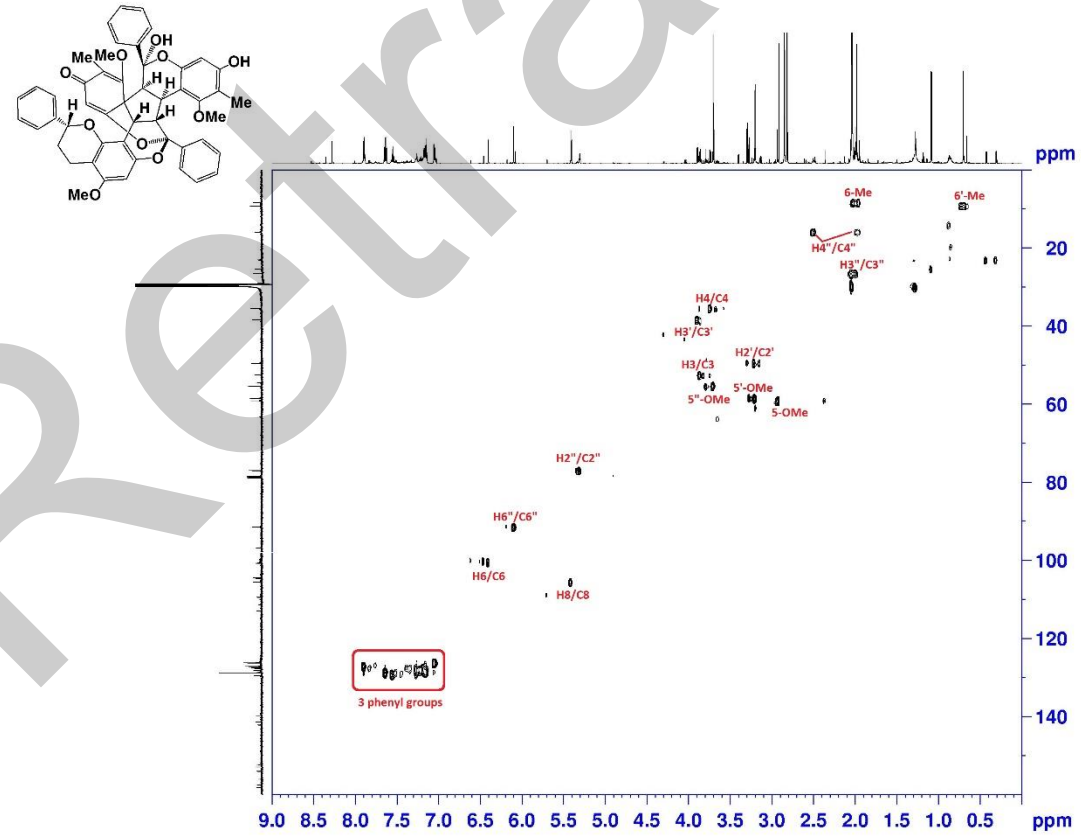

Fig. S23. HMBC spectrum of **2** in d_6-Acetone (^{1}H-^{13}C: 700 MHz)

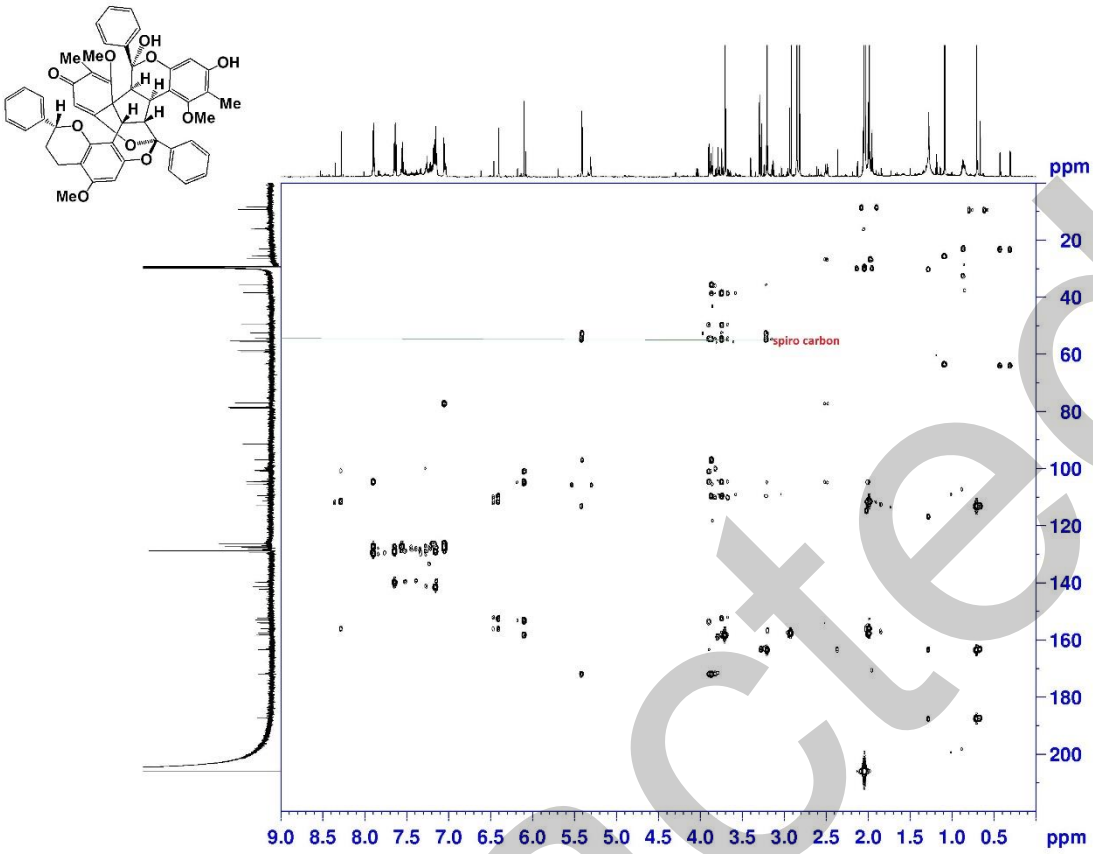

Fig. S24. Key NOESY spectrum of **2** in $CDCl_3$ (^1H-^1H: 700 MHz)

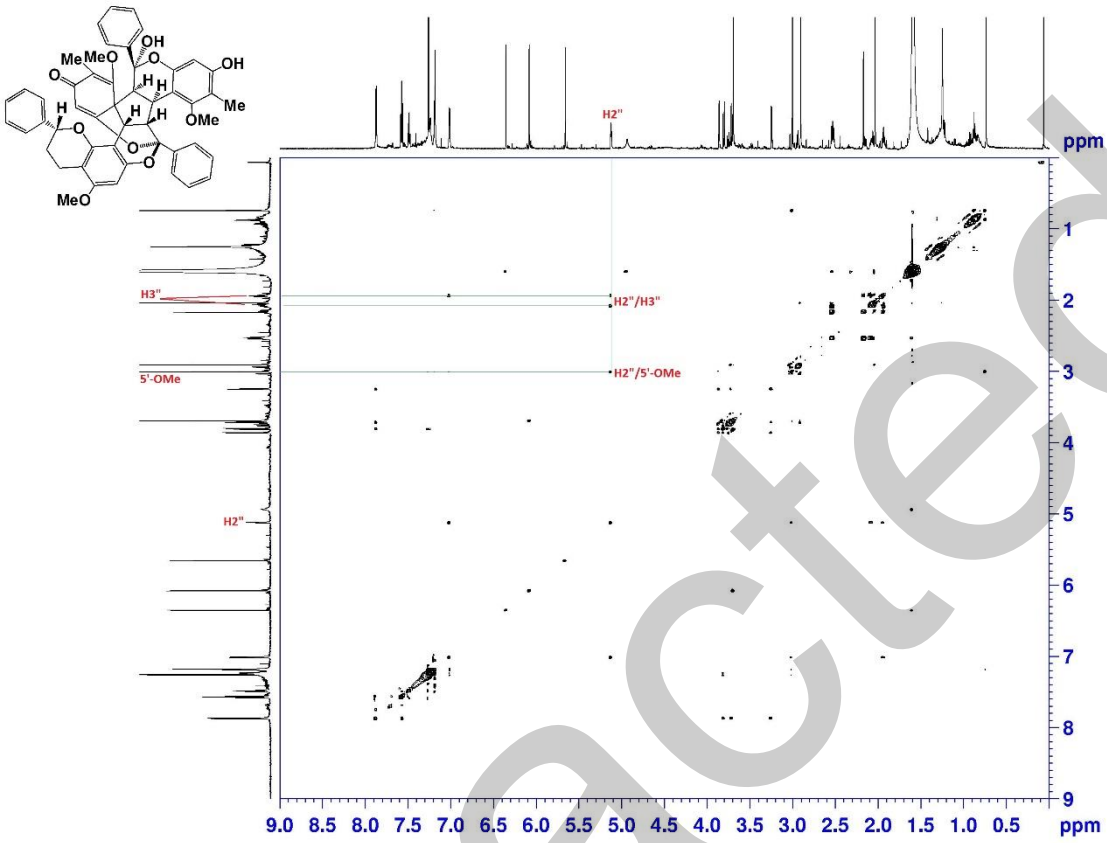

Fig. S25. H2″&6′-Me had NOE on 3.4Å (A1, green); had no NOE on 6.3Å for A2 (red).

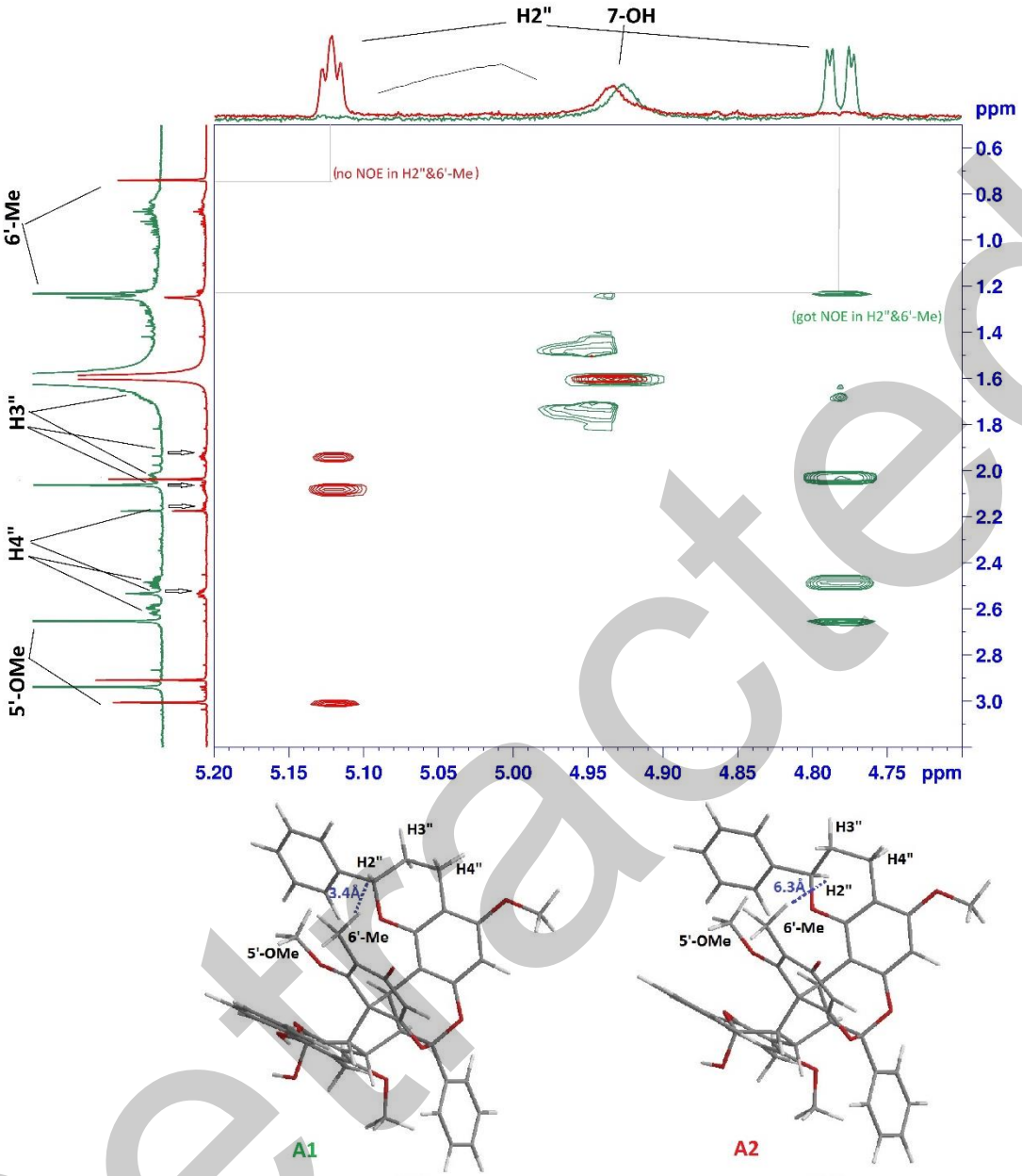

Fig. S26. A1 and A2 would transform to other compounds (quick-dry: collected and then concentrated soon after per inject by chiral-HPLC) shown in ^{1}H-NMR in d_6-acetone.

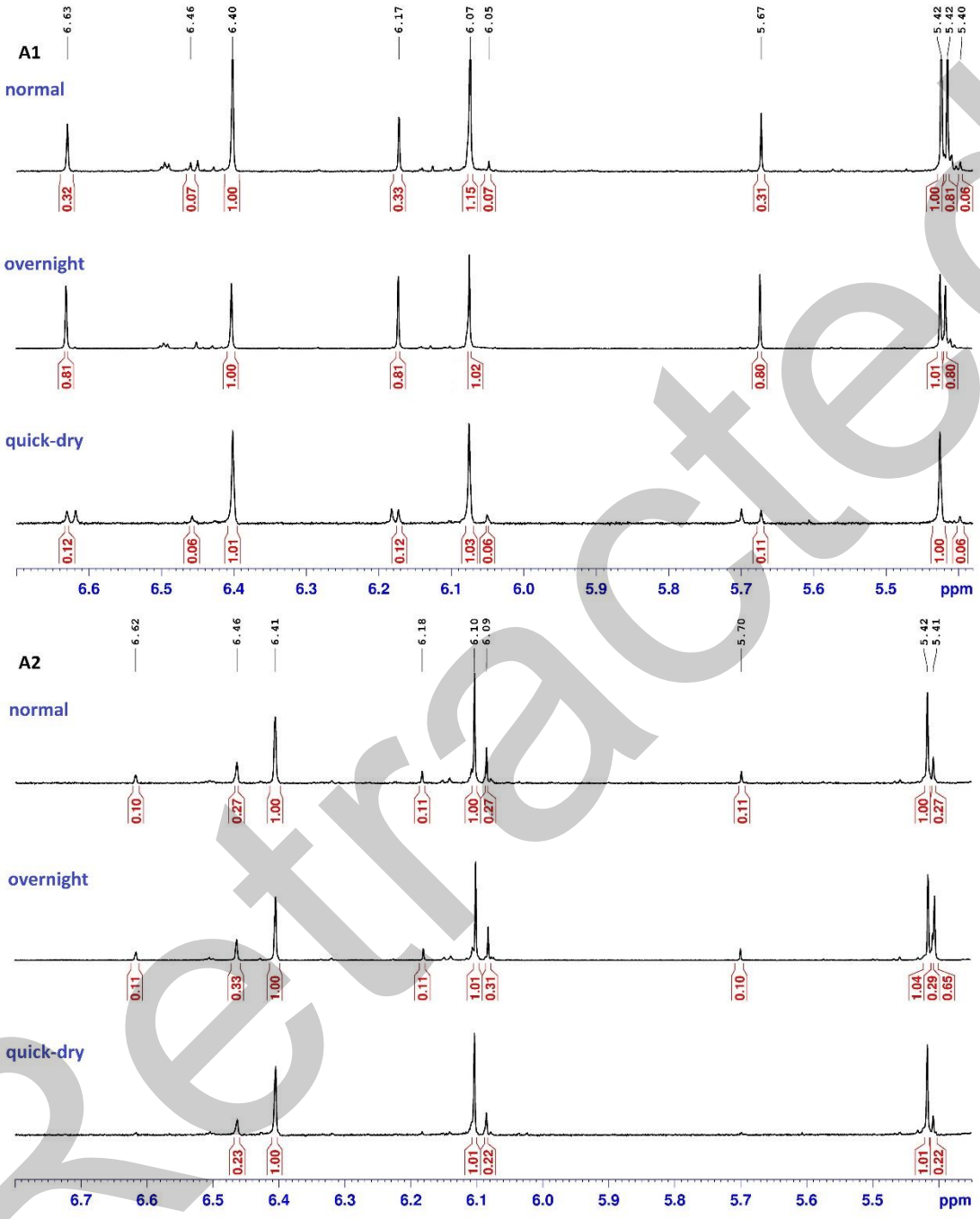

Fig. S27 Biosynthetic pathway of **1** and **2**

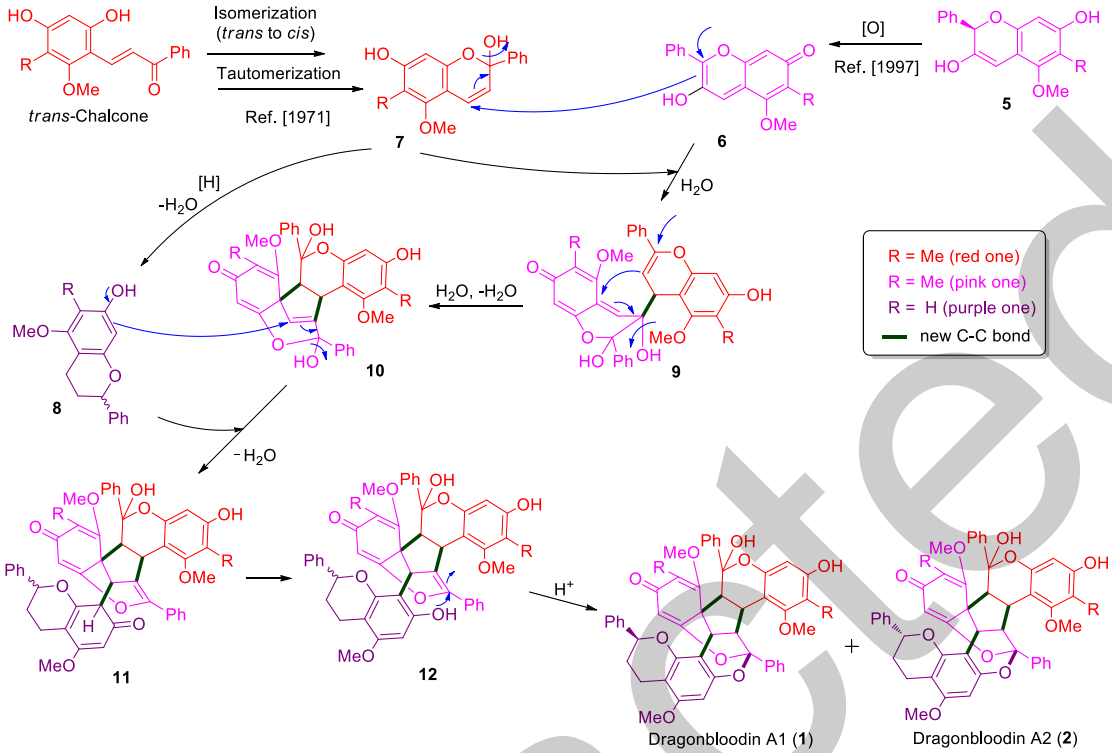

Fig. S28 Effects of dragonbloodin A1 (**1**) on the activities human neutrophil elastase in cell-free system. All data are expressed as the mean ± S.E.M. (n = 3).

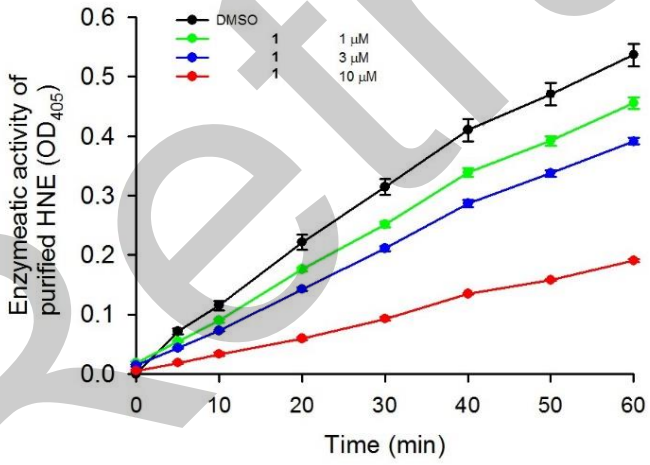

Fig. S29 Effects of dragonbloodin A2 (**2**) on the activities human neutrophil elastase in cell-free system. All data are expressed as the mean ± S.E.M. (n = 3).